

Genetic paths to evolutionary rescue and the distribution of fitness effects along them

Matthew M Osmond^{*,1}, Sarah P Otto^{*} and Guillaume Martin[†]

^{*}Biodiversity Centre & Department of Zoology, University of British Columbia, [†]Institut des Sciences de l'Evolution de Montpellier, Université Montpellier II

1 ABSTRACT

2 The past century has seen substantial theoretical and empirical progress on the genetic basis of adaptation. Over this same period a pressing need to prevent the evolution of drug resistance has uncovered much about the potential genetic basis of persistence in declining populations. However, we have little theory to predict and generalize how persistence – by sufficiently rapid adaptation – might be realized in this explicitly demographic scenario. Here we use Fisher's geometric model with absolute fitness to begin a line of theoretical inquiry into the genetic basis of evolutionary rescue, focusing here on asexual populations that adapt through *de novo* mutations. We show how the dominant genetic path to rescue switches from a single mutation to multiple as mutation rates and the severity of the environmental change increase. In multi-step rescue, intermediate genotypes that themselves go extinct provide a 'springboard' to rescue genotypes. Comparing to a scenario where persistence is assured, our approach allows us to quantify how a race between evolution and extinction leads to a genetic basis of adaptation that is composed of fewer loci of larger effect. We hope this work brings awareness to the impact of demography on the genetic basis of adaptation.

13 **KEYWORDS** Antimicrobial drug resistance; Evolutionary escape; Fisher's geometric model; Genetic basis of adaptation; Mathematical theory

14 Our understanding of the genetic basis of adaptation is 33 rapidly improving due to the now widespread use of genomic sequencing (see examples in Bell 2009; Stapley *et al.* 2010; 34 Dettman *et al.* 2012; Schlötterer *et al.* 2015). A recurrent observation, especially in experimental evolution with asexual microbes, 35 is that the more novel the environment and the stronger the selection pressure, the more likely it is that adaptation primarily 36 proceeds by fewer mutations of larger effect (i.e., that adaptation 37 is oligogenic *sensu* Bell 2009). An extreme case is the evolution 38 of drug resistance, which is often achieved by just one or two 39 mutations (e.g., Bataillon *et al.* 2011; Pennings *et al.* 2014).

40 However, drugs, and other sufficiently novel environments, 41 will often induce not only strong selection but also population 42 decline. Such declines hinder both the production and maintenance 43 of adaptive genetic variation (Otto and Whitlock 1997), 44 thus impeding evolution and threatening extinction. Drug 45 resistance evolution is a particular instance of the more general 46 phenomenon of evolutionary rescue (Gomulkiewicz and Holt 47

48 1995; Bell 2017), where persistence requires sufficiently fast adaptive evolution.

49 Most theory on the genetics of adaptation (reviewed in Orr 50 2005) assumes constant population size and therefore does not 51 capture the characteristic 'race' between adaptation and extinction 52 that occurs during evolutionary rescue. Many models have 53 been created to describe this race (reviewed in Alexander *et al.* 54 2014) but so far largely focus on two extreme genetic bases, both 55 already introduced in Gomulkiewicz and Holt (1995): rescue 56 is either caused by minute changes in allele frequencies across 57 many loci in sexuals (i.e., the infinitesimal model; Fisher 1918) or 58 by the substitution of a single large effect 'resistance' mutation 59 (e.g., one locus, two allele models). We therefore largely lack 60 a theoretical framework for the genetic basis of evolutionary 61 rescue that captures the arguably more realistic situation where 62 an intermediate number of mutations are at play (but see exceptions 63 below). The near absence of such a framework prevents us 64 from predicting the number of mutations that evolutionary 65 rescue will take and the distribution of their effect sizes. The 66 existence of a more complete framework could therefore provide 67 valuable information for those investigating the genetic basis 68 of drug resistance (e.g., the expected number and effect sizes of

55 mutations) and would extend our understanding of the genetic
56 basis of adaptation to cases of non-equilibrium demography (i.e.,
57 rapid evolution and "eco-evo" dynamics).

58 Despite these gaps in the theory on the genetic basis of evolutionary
59 rescue, there is a wealth of data. For example, the genetic
60 basis of resistance to a variety of drugs is known in many species
61 of bacteria (reviewed in [MacLean et al. 2010](#)), fungi (reviewed
62 in [Robbins et al. 2017](#)), and viruses (reviewed in [Yilmaz et al.](#)
63 [2016](#)). This abundance of data reflects both the applied need
64 to prevent drug resistance and the relative ease of isolating the
65 genotypes that survive (hereafter "rescue genotypes"), e.g., in
66 a Luria-Delbrück fluctuation assay (reviewed in [Bataillon and](#)
67 [Bailey 2014](#)). Assaying fitness in the environment used to isolate
68 mutants (e.g., in the drug) then provides the distribution of fit-
69 ness effects of potential rescue genotypes. Additional data on
70 the genetic basis of drug resistance arise from the construction
71 of mutant libraries (e.g., [Weinreich et al. 2006](#)) and the sequenc-
72 ing of natural populations (e.g., [Pennings et al. 2014](#)). Together,
73 the data show that resistance often appears to arise by a single
74 mutation (e.g., [MacLean and Buckling 2009](#); [Lindsey et al. 2013](#);
75 [Gerstein et al. 2012](#)) but not always (e.g., [Bataillon et al. 2011](#);
76 [Pennings et al. 2014](#); [Gerstein et al. 2015](#); [Williams and Pennings](#)
77 [2019](#)). The data also indicate that the fitness effect of rescue geno-
78 types is more often large than small, creating a hump-shaped
79 distribution of selection coefficients (e.g., [Kassen and Bataillon](#)
80 [2006](#); [MacLean and Buckling 2009](#); [Gerstein et al. 2012](#); [Lindsey](#)
81 [et al. 2013](#); [Gerstein et al. 2015](#)) that is similar in shape to that
82 proposed by [Kimura \(1983\)](#) (see [Orr 1998](#), for more discussion)
83 but with a lower bound that is often much greater than zero.

84 Theory on evolutionary rescue (reviewed in [Alexander et al.](#)
85 [2014](#)) has primarily focused on the probability of rescue rather
86 than its genetic basis. However, a few studies have varied the
87 potential genetic basis enough to make some inference about
88 how evolutionary rescue is likely to happen. For instance, in the
89 context of pathogen host-switching, [Antia et al. \(2003\)](#) numer-
90 ically explored the probability of rescue starting from a single
91 ancestral individual when k sequential mutations are required
92 for a positive growth rate, each mutation occurring from the
93 previous genotype with the same probability and all interme-
94 diate genotypes being selectively neutral. The authors found that
95 rescue became less likely as the number of intermediate muta-
96 tions increased, suggesting that rescue will generally proceed by
97 the fewest possible mutations. This framework was expanded
98 greatly by [Iwasa et al. \(2004a\)](#), who allowed for arbitrary muta-
99 tional networks (i.e., different mutation rates between any two
100 genotypes) and standing genetic variation in the ancestral popu-
101 lation. Assuming the probability of mutation between any two
102 genotypes is of the same order, they showed that genetic paths
103 with fewer mutational steps contributed more to the total proba-
104 bility of rescue, again suggesting rescue will occur by the fewest
105 possible mutations. [Iwasa et al. \(2004a\)](#) also found that multiple
106 simultaneous mutations (i.e., arising in the same meiosis) can
107 contribute more to rescue than paths that gain these same mu-
108 tations sequentially (i.e., over multiple generations) when the
109 growth rates of the intermediate mutations are small enough,
110 suggesting that rare large mutations can be the most likely path
111 to rescue when the population is very maladapted or there is a
112 fitness valley separating the wildtype and rescue genotype. This
113 point was also demonstrated by [Alexander and Day \(2010\)](#), who
114 emphasized that multiple simultaneous mutations become the
115 dominant path to rescue in the most challenging environments.
116 As a counterpoint, [Uecker and Hermisson \(2016\)](#) explored a

117 greater range of fitness values in a two-locus two-allele model,
118 showing that, with standing genetic variation, rescue by sequen-
119 tial mutations at two loci (two mutational steps) can be more
120 likely than rescue by mutation at a single locus (one simulta-
121 neous mutational step), particularly when the wildtype is very
122 maladapted, where the single mutants can act as a buffer in
123 the face of environmental change. In summary, current theory
124 indicates that the genetic basis of rescue hinges on the chosen
125 set of genotypes, their fitnesses, and the mutation rates between
126 them. So far these choices have been in large part arbitrary or
127 chosen for mathematical convenience.

128 Here we follow the lead of [Anciaux et al. \(2018\)](#) in allowing
129 the genotypes that contribute to rescue, as well as their fitnesses
130 and the mutational distribution, to arise from an empirically-
131 justified fitness-landscape model ([Tenaillon 2014](#)). In particular,
132 we use Fisher's geometric model to describe adaptation follow-
133 ing an abrupt environmental change that instigates population
134 decline. There are two key differences between this approach
135 and earlier models using Fisher's geometric model (e.g., [Orr](#)
136 [1998](#)): here 1) the dynamics of each genotype depends on their
137 absolute fitness (instead of only on their relative fitness) and 2)
138 multiple mutations can segregate simultaneously (instead of as-
139 suming only sequential fixation), allowing multiple mutations to
140 fix – and in our case, rescue the population – together as a single
141 haplotype (i.e., stochastic tunnelling, [Iwasa et al. 2004b](#)). In this
142 non-equilibrium scenario, variation in absolute fitness, which
143 allows population size to vary, can create feedbacks between
144 demography and evolution, which could strongly impact the
145 genetic basis of adaptation relative to the constant population
146 size case. In contrast to [Anciaux et al. \(2018\)](#), our focus here is
147 on the genetic basis of evolutionary rescue and we also explore
148 the possibility of rescue by mutant haplotypes containing more
149 than one mutation. In particular, we ask: (1) How many muta-
150 tional steps is evolutionary rescue likely to take? and (2) What
151 is the expected distribution of fitness effects of the surviving
152 genotypes and their component mutations?

153 We first introduce the modelling framework before summa-
154 rizing our main results. We then present the mathematical anal-
155 yses we have used to understand these results and end with a
156 discussion of our key findings.

157 **Data availability**

158 Code used to derive analytical and numerical results and pro-
159 duce figures (referred to here as File S1; *Mathematica*, ver-
160 sion 9.0; [Wolfram Research Inc. 2012](#)) and code used to create
161 individual-based simulation data (Python, version 3.5; Python
162 Software Foundation), as well as simulation data and freely
163 accessible versions of File S1 (CDF and PDF), are available at
164 <https://github.com/mmosmond/GeneticBasisOfRescue>.

165 **Model**

166 **Fisher's geometric model**

167 We map genotype to phenotype to fitness using Fisher's geo-
168 metric model, originally introduced by Fisher ([1930](#), p. 38-41)
169 and reviewed by [Tenaillon \(2014\)](#). In this model each geno-
170 type is characterized by a point in n -dimensional phenotypic
171 space, \vec{z} . We ignore environmental effects, and thus the phe-
172 notype is the breeding value. At any given time there is a
173 phenotype, \vec{o} , that has maximum fitness and fitness declines
174 monotonically as phenotypes depart from \vec{o} . We assume that
175 n phenotypic axes can be chosen and scaled such that fitness

is described by a multivariate Gaussian function with variance 1 in each dimension, no covariance, and height W_{max} (which can always be done when considering genotypes close enough to an non-degenerate optimum; [Martin 2014](#)). Thus the fitness of phenotype \vec{z} is $W(\vec{z}) = W_{max} \exp(-||\vec{z} - \vec{o}||^2/2)$, where $||\vec{z} - \vec{o}|| = \sqrt{\sum_{i=1}^n (z_i - o_i)^2}$ is the Euclidean distance of \vec{z} from the optimum, \vec{o} . Here we are interested in absolute fitness; we take $\ln[W(\vec{z})] = m(\vec{z}) = m_{max} - ||\vec{z} - \vec{o}||^2/2$ to be the continuous-time growth rate (m is for Malthusian fitness) of phenotype \vec{z} . We ignore density- and frequency-dependence in $m(\vec{z})$ for simplicity. The fitness effect, i.e., selection coefficient, of phenotype z' relative to z in a continuous-time model is exactly $s = \log[W(z')/W(z)] = m(z') - m(z)$ ([Martin and Lenormand 2015](#)). This is approximately equal to the selection coefficient in discrete time $(W(z')/W(z) - 1)$ when selection is weak ($W(z') - W(z) \ll 1$).

To make analytical progress we use the isotropic version of Fisher's geometric model, where mutations (in addition to selection) are assumed to be uncorrelated across the scaled traits. Universal pleiotropy is also assumed, so that each mutation affects all scaled phenotypes. In particular we use the "classic" form of Fisher's geometric model ([Harmand et al. 2017](#)), where the probability density function of a mutant phenotype is multivariate normal, centred on the current phenotype, with variance λ in each dimension and no covariance. Using a probability density function of mutant phenotypes implies a continuum-of-alleles ([Kimura 1965](#)), i.e., phenotype is continuous and each mutation is unique. Mutations are assumed to be additive in phenotype, which induces epistasis in fitness (as well as dominance under diploid selection), as fitness is a non-linear function of phenotype. We assume asexual reproduction, i.e., no recombination, which is appropriate for many cases of antimicrobial drug resistance and experimental evolution, while recognizing the value of expanding this work to sexual populations.

An obvious and important extension would be to relax the simplifying assumptions of isotropy and universal pleiotropy, which we leave for future work. Note that mild anisotropy yields the same bulk distribution of fitness effects as an isotropic model with fewer dimensions ([Martin and Lenormand 2006](#)), but this does not extend to the tails of the distribution. Therefore, whether anisotropy can be reduced to isotropy with fewer dimensions in the case of evolutionary rescue, where the tails are essential, is unknown. In the [Discussion](#) we briefly explore the effects of non-Gaussian distributions of mutant phenotypes.

Given this phenotype-to-fitness mapping and phenotypic distribution of new mutations, the distribution of fitness effects (and therefore growth rates) of new mutations can be derived exactly. Let m be the growth rate of some particular focal genotype and m' the growth rate of a mutant immediately derived from it. Then let $s_0 = m_{max} - m$ be the selective effect of a mutant with the optimum genotype and $s = m' - m$ the selective effect of the mutant with growth rate m' . The probability density function of the selective effects of new mutations, s , is then given by equation 3 in [Martin and Lenormand \(2015\)](#). Converting fitness effects to growth rate ($m' = s + m$), the probability density function for mutant growth rate m' from an ancestor with growth rate m is (cf. equation 2 in [Anciaux et al. 2018](#))

$$f(m'|m) = \frac{2}{\lambda} f_{\chi_n^2} \left(\frac{2(m_{max} - m')}{\lambda}, \frac{2(m_{max} - m)}{\lambda} \right), \quad (1)$$

where $f_{\chi_n^2}(x, c)$ is the probability density function over positive

real numbers x of $\chi_n^2(c)$, a non-central chi-square deviate with n degrees of freedom and noncentrality $c > 0$ (equation 26.4.25 in [Abramowitz and Stegun 1972](#)).

Lifecycle

We are envisioning a scenario where N_0 wildtype individuals, each of which have phenotype \vec{z}_0 , experience an environmental change, causing population decline, $m_0 \equiv m(\vec{z}_0) < 0$. Each generation, an individual with phenotype \vec{z} produces a Poisson number of offspring, with mean $\ln[m(\vec{z})]$, and dies. This process implicitly assumes no interaction between individuals, i.e., a branching process with density- and frequency-independent growth and fitness and no clonal interference. Each offspring mutates with probability U (we ignore the possibility of multiple simultaneous mutations within a single genome), and mutations are distributed as described above (see [Fisher's geometric model](#)).

Simulation procedure

We ran individual-based simulations of the above process to compare with our numeric and analytic results. Populations were considered rescued when there were ≥ 1000 individuals (Figures 1-3) or ≥ 100 individuals (Figures 6-7, S1, and S3) with positive growth rates (all other replicates went extinct). The most common genotype at the time of rescue was considered the rescue genotype, and the number of mutational steps to rescue was set as the number of mutations in that genotype.

Probability of rescue

Let p_0 be the probability that a given wildtype individual is "successful", i.e., has descendants that rescue the population. The probability of rescue is then one minus the probability that none of the initial wildtype individuals are successful,

$$P = 1 - (1 - p_0)^{N_0} \approx 1 - \exp(-N_0 p_0), \quad (2)$$

where the approximation assumes small p_0 and large N_0 . What remains is to find p_0 .

Summary of Results

We start with a heuristic explanation of our main results before turning to more detailed derivations in the next section.

Rescue by multiple mutations

A characteristic pattern of evolutionary rescue is a "U"-shaped population size trajectory (e.g., [Orr and Unckless 2014](#)). This is the result of an exponentially-declining wildtype genotype being replaced by an exponentially-increasing mutant genotype. On a log scale this population size trajectory becomes "V"-shaped (we denote it a 'V-shaped log-trajectory'). On this scale, the population declines at a constant rate (producing a line with slope $m_0 < 0$) until the growing mutant subpopulation becomes relatively common, at which point the population begins growing at a constant rate (a line with slope $m_1 > 0$). This characteristic V-shaped log-trajectory is observed in many of our simulations where evolutionary rescue occurs (Figure 1A). Alternatively, when the wildtype declines faster and the mutation rate is larger we sometimes see 'U-shaped log-trajectories' (e.g., the red and blue replicates in Figure 2A). Here there are three phases instead of two; the initial rate of decline (a line with slope $m_0 < 0$) is first reduced (transitioning to a line with slope $m_1 < 0$) before the population begins growing (a line with slope $m_2 > 0$).

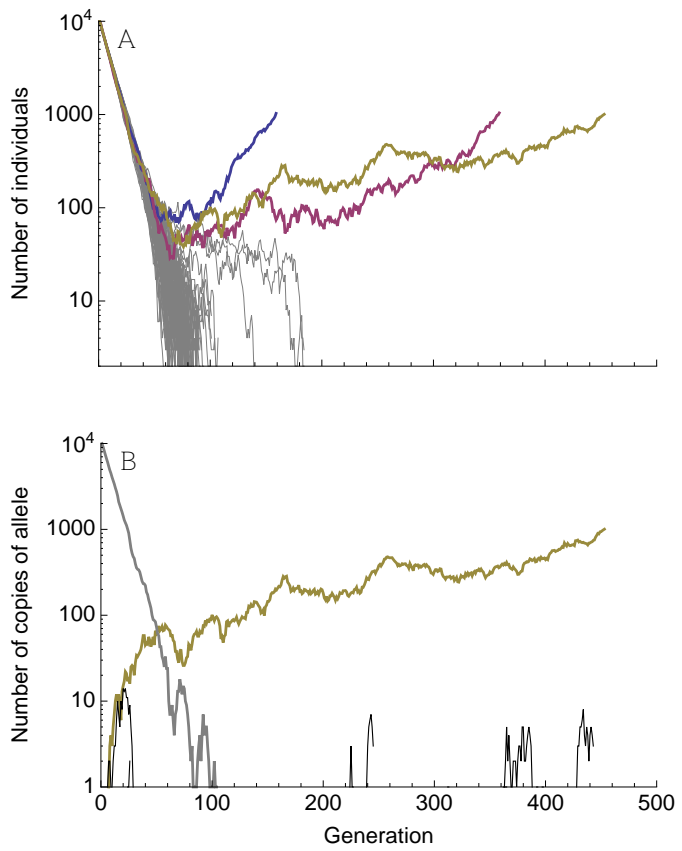


Figure 1 Typical dynamics with a relatively slow wildtype decline and a small mutation rate ($m_0 = -0.1, U = 10^{-4}$). **(A)** Population size trajectories on a log scale. Each line is a unique replicate simulation (100 replicates). Replicates that went extinct are grey, replicates that were rescued are in colour (and are roughly V-shaped). **(B)** The number of individuals with a given derived allele, again on a log scale, for the yellow replicate in A. The number of individuals without any derived alleles (wildtypes) is shown in grey, the rescue mutation is shown in yellow, and all other mutations are shown in black. Other parameters: $n = 4, \lambda = 0.005, m_{max} = 0.5$.

As expected, V-shaped log-trajectories are the result of a single mutation creating a genotype with a positive growth rate that escapes loss when rare and rescues the population (Figure 1B), i.e., 1-step rescue. U-shaped log-trajectories, on the other hand, occur when a single mutation creates a genotype with a negative (or potentially very small positive) growth rate, itself doomed to extinction, which out-persists the wildtype and gives rise to a double mutant genotype that rescues the population (Figure 2B), i.e., 2-step rescue. These two types of rescue comprise the overwhelming majority of rescue events observed in our simulations, across a wide range of wildtype decline rates (e.g., Figure 3).

In the text, we focus on low to moderate mutation rates affecting growth rate. With sufficiently high mutation rates rescue by 3 or more mutations comes to dominate (Figure S1). It has recently been suggested that when the mutation rate, U , is substantially less than a critical value, $U_C = \lambda n^2 / 4$, we are in a "strong selection, weak mutation" regime where selection is strong enough relative to mutation that essentially all mutations arise on a wildtype background (Martin and Roques 2016), con-

sistent with the House of Cards approximation (Turelli 1984, 1985). Thus in this regime rescue tends to occur by a single mutation of large effect (Anciaux *et al.* 2018). In the other extreme, when $U > U_C$, we are in a "weak selection, strong mutation" regime where selection is weak enough relative to mutation that many cosegregating mutations are present within each genome, creating a multivariate normal phenotypic distribution (Martin and Roques 2016), consistent with the Gaussian approximation (Kimura 1965; Lande 1980). Thus in this regime rescue tends to occur by many mutations of small effect (Anciaux *et al.* 2019). As shown in Figure 3 (where $U = U_C/10$) and Figure S1 (where $U_C = 0.02$), rescue by a small number of mutations (but more than one) can become commonplace in the transition zone (where U is neither much smaller or much larger than U_C), where there are often a considerable number of cosegregating mutations (e.g., Figure 2B, where $U = U_C/2$).

The probability of k -step rescue

Approximations for the probability of 1-step rescue under the strong selection, weak mutation regime were derived by Anciaux *et al.* (2018). Here we extend this study by exploring the contribution of k -step rescue, deriving approximations for the probability of such events, as well as dissecting the genetic basis of both 1- and 2-step rescue in terms of the distribution of fitness effects of rescue genotypes and their component mutations.

Although requiring a sufficiently beneficial mutation to arise on a rare mutant genotype doomed to extinction, multi-step evolutionary rescue can be the dominant form of rescue when the wildtype is sufficiently maladapted (Figures 3 and S1). Indeed, on this fitness landscape, the probability of producing a rescue genotype in one mutational step mutant drops very sharply with maladaptation (Anciaux *et al.* 2018); the probability of multi-step rescue declines more slowly as mutants with intermediate growth rates can be a "springboard" – albeit not always a very bouncy one – from which rescue mutants are produced. These intermediates contribute more as mutation rates and the decline rate of the wildtype increase (Figures 3 and S1), the former because double mutants become more likely and the latter because the springboard becomes more necessary. With a large enough number of wildtype individuals or a high enough mutation rate (Figure S1), multi-step rescue can not only be more likely than 1-step, but also very likely in an absolute sense.

Classifying 2-step rescue regimes

2-step rescue can occur through first-step mutants with a wide range of growth rates. As shown below (see Approximating the probability of 2-step rescue), these first-step mutants can be divided into three regimes: "sufficiently subcritical", "sufficiently critical", and "sufficiently supercritical" (we will often drop "sufficiently" for brevity; Figure 4). Sufficiently critical first-step mutants are defined by having growth rates close enough to zero that the most likely way for such a mutation to lead to 2-step rescue is for it to persist for such an unusually long period of time, and accordingly grow to such an unusually large subpopulation size, that it will almost certainly produce successful double mutants. Sufficiently subcritical first-step mutants are then defined by having growth rates that are negative enough to almost certainly prevent such long persistence times. Instead, these mutations tend to persist for an expected number of generations, proportional to the inverse of their growth rate ($1/|m|$), while maintaining relatively small subpopulation sizes (on the order of one individual per generation). Mutations conferring

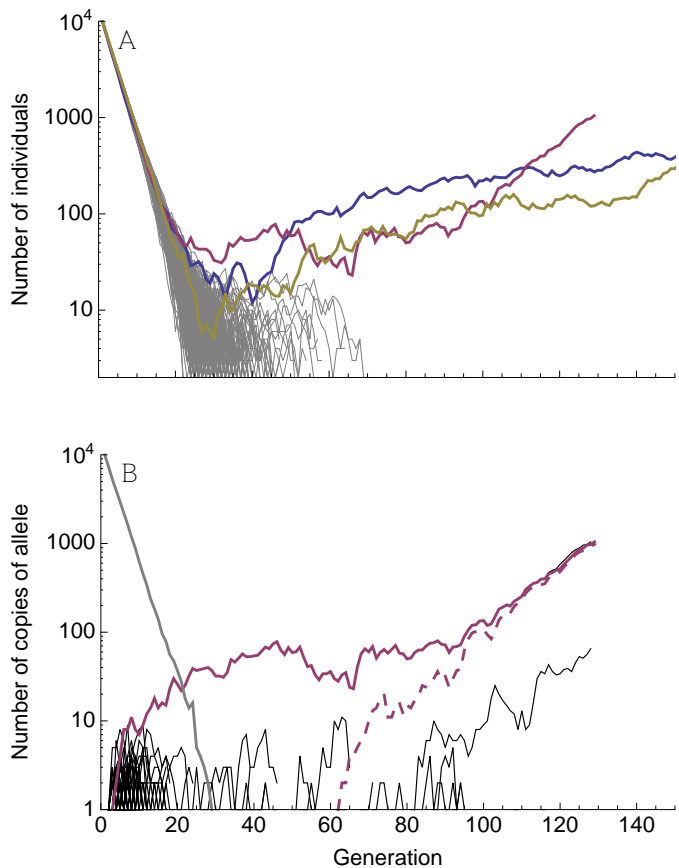


Figure 2 Typical dynamics with a relatively fast wildtype decline and a large mutation rate ($m_0 = -0.3, U = 10^{-2}$). **(A)** Population size trajectories on a log scale. Each line is a unique replicate simulation (500 replicates). Replicates that went extinct are grey, replicates that were rescued are in colour. Note that the blue and red replicates are cases of 2-step rescue (and roughly U-shaped), while the yellow replicate is 1-step rescue (and therefore V-shaped). **(B)** The number of individuals with a given derived allele, again on a log scale, for the red replicate in A. The number of individuals without any derived alleles (wildtypes) is shown in grey, the rescue mutations are shown in red, and all other mutations in black. Here a single mutant with growth rate less than zero arises early and outlives the wildtype (solid red). A second mutation then arises on that background (dashed red), making a double mutant with a growth rate greater than zero that rescues the population. Other parameters: $n = 4, \lambda = 0.005, m_{max} = 0.5$.

381 not 1-step rescue with subsequent adaptation as we condition
 382 on the first-step mutation going extinct in the absence of the
 383 second mutation. However, empirically it will be impossible
 384 to tell if the first-step mutation was indeed doomed to extinction
 385 if it is found to have a positive growth rate in the selective
 386 environment.

387 The relative contribution of each regime changes with both
 388 the initial degree of maladaptation and the mutation rate (Fig-
 389 ures 5 and S2). When the wildtype is very maladapted (relative
 390 to mutational variance), most 2-step rescue events occur through
 391 subcritical first-step mutants (Figure 5A), which arise at a higher
 392 rate than critical or supercritical mutants and yet persist longer
 393 than the wildtype. When the wildtype is less maladapted, how-
 394 ever, critical and supercritical mutations become increasingly
 395 likely to arise and contribute to 2-step rescue, both due to their
 396 closer proximity to the wildtype in phenotypic space as well
 397 as the slower decline of the wildtype increasing the cumulative
 398 number of mutations that occur. The mutation rate also plays
 399 an interesting role in determining the relative contributions of
 400 each regime (Figures 5B and S2). When mutations are rare, only
 401 first-step mutations that are very nearly neutral ($m \sim 0$) will
 402 persist long enough to give rise to a 2-step rescue mutation. As
 403 the mutation rate increases, however, the range of first-step mu-
 404 tant growth rates that can persist long enough to lead to 2-step
 405 rescue widens because fewer individuals carrying the first-step
 406 mutation are needed before a successful double mutant arises.

407 **The distribution of fitness effects among rescue mutations**

408 Mutants causing 1-step rescue have growth rates that cluster
 409 around small positive values ($m \gtrsim 0$; blue curves in Figure 6).
 410 Consequently, the distribution of fitness effects (DFE) among
 411 these rescue mutants is shifted to the right relative to mutations
 412 that establish in a population of constant size (compare solid
 413 blue and gray curves in Figure 6), with a DFE beginning at
 414 $s = m - m_0 \geq -m_0 > 0$ rather than $s = 0$ (Kimura 1983). As a
 415 result of this increased threshold, the 1-step rescue DFE has a
 416 smaller variance than both the DFE of random mutations and
 417 the DFE of mutations that establish in a constant population
 418 (compare blue and gray curves in Figure 6). Further, while the
 419 variance in the DFE of random mutations and of those that
 420 establish in a population of constant size increases slightly with
 421 initial maladaptation (due to the curvature of the phenotype-to-
 422 fitness function), the variance in the 1-step rescue DFE decreases
 423 substantially (compare panels in Figure 6), as rescue becomes
 424 restricted to a rapidly decreasing proportion of the available
 425 mutants.

426 The DFE of genotypes that cause 2-step rescue (the combined
 427 effect of two mutations) is also clustered at small positive growth
 428 rates, but it has a variance that is less affected by the rate of wild-
 429 type decline (red curves in Figure 6). This is because double
 430 mutant rescue genotypes are created via first-step mutant geno-
 431 types that have larger growth rates than the wildtype (i.e., are
 432 closer to the optimum), allowing them to create double mutants
 433 with a larger range of positive growth rates.

434 Finally, we can also look at the distribution of growth rates
 435 among first-step mutations that lead to 2-step rescue, i.e., 'spring-
 436 board mutants' (Figures 7 and S2). Here there are two main
 437 factors to consider: 1) the probability that a mutation with a
 438 given growth rate arises on the wildtype background but does
 439 not by itself rescue the population and 2) the probability that
 440 such a mutation persists long enough for a sufficiently beneficial
 441 second mutation to arise on that same background and together

368 a positive growth rate can also go extinct, and thus can also
 369 act as springboards to rescue. Conditioned on extinction, su-
 370 percritical mutations behave like subcritical mutations with a
 371 growth rate of the same absolute value (Maruyama and Kimura
 372 1974). Sufficiently supercritical first-step mutants are therefore
 373 defined analogously to subcritical first-step mutants, having pos-
 374 itive (rather than negative) growth rates that are large enough
 375 to prevent sufficiently long persistence times once conditioned
 376 on extinction. Despite having similar extinction trajectories as
 377 subcritical mutations, 'doomed' supercritical mutations arise
 378 less frequently by mutation from the wildtype but mutate to res-
 379 cue genotypes at a higher rate. Overall, they too can contribute
 380 substantially to rescue. Note that supercritical 2-step rescue is

442 rescue the population. Subcritical mutations conferring growth
 443 rates closer to zero persist longer but are less likely to arise from
 444 the wildtype, creating a trade-off between mutational input and
 445 the probability of rescue that can lead to a wide distribution
 446 of contributing subcritical growth rates (blue shading in Fig-
 447 ure 7). In contrast, supercritical mutations with growth rates
 448 nearer to zero are more likely to arise by mutation, to go extinct in
 449 the absence of further mutation, and to persist for longer once
 450 conditioned on extinction, together creating a relatively narrow
 451 distribution of contributing supercritical growth rates (yellow
 452 shading in Figure 7). As explained above, increasing the rate of
 453 wildtype decline (or decreasing the rate of mutation) increases
 454 the contribution of subcritical first-step mutants and the impor-
 455 tance of mutational input, lowering the mode and increasing the
 456 variance of the first-step DFE (compare panels in Figure 7).

457 Note that, given 2-step rescue, the growth rate of both the
 458 first-step and second-step mutation may be negative when con-
 459 sidered by themselves in the wildtype background. This poten-
 460 tially obscures empirical detection of the individual mutations
 461 involved in evolutionary rescue.

462 Mathematical Analysis

463 The probability of k -step rescue

464 Generic expressions for the probability of 1- and 2-step rescue
 465 were given by [Martin et al. \(2013\)](#), using a diffusion approxima-
 466 tion of the underlying demographics. The key result that we
 467 will use is the probability that a single copy of a genotype with
 468 growth rate m , itself fated for extinction but which produces
 469 rescue mutants at rate $\Lambda(m)$, rescues the population (equation
 470 S1.5 in [Martin et al. 2013](#)). With our lifecycle this is (c.f., equation
 471 A.3 in [Iwasa et al. 2004a](#))

$$p(m, \Lambda(m)) = 1 - \exp \left[|m| \left(1 - \sqrt{1 + \frac{2\Lambda(m)}{m^2}} \right) \right]. \quad (3)$$

472 We can therefore use $p_0 = p(m_0, \Lambda(m_0))$ as the probability that a
 473 wildtype individual has descendants that rescue the population
 474 and what remains in calculating the total probability of rescue
 475 (Equation 2) is $\Lambda(m_0)$. We break this down by letting $\Lambda_i(m)$ be
 476 the rate at which rescue genotypes with i mutations are created;
 477 the total probability of rescue is then given by Equation 2 with
 478 $p_0 = p(m_0, \sum_{i=1}^{\infty} \Lambda_i(m_0))$.

479 In 1-step rescue, $\Lambda_1(m_0)$ is just the rate of production of res-
 480 cue mutants directly from a wildtype genotype. This is the
 481 probability that a wildtype gives rise to a mutant with growth
 482 rate m (given by $Uf(m|m_0)$) times the probability that a geno-
 483 type with growth rate m establishes. Again approximating our
 484 discrete time process with a diffusion process, the probability
 485 that a lineage with growth rate $m << 1$ establishes, ignoring
 486 further mutation, is (e.g., [Martin et al. 2013](#))

$$p_{est}(m) \approx \begin{cases} 0 & m \leq 0 \\ 1 - \exp(-2m) & m > 0 \end{cases}. \quad (4)$$

487 This reduces to the $2(s + m_0)$ result in [Otto and Whitlock \(1997\)](#)
 488 when $m = s + m_0$ is small, which further reduces to $2s$ in a
 489 population of constant size, where $m_0 = 0$ ([Haldane 1927](#)). Using
 490 this, the rate of 1-step rescue is

$$\Lambda_1(m_0) = U \int_0^{m_{max}} f(m|m_0) p_{est}(m) dm. \quad (5)$$

Symbol	Meaning
n	number of (scaled) phenotypic dimensions
λ	variance in mutant phenotypes along each dimension
m_{max}	maximum growth rate
$f(m' m)$	distribution of growth rates among mutants from a genotype with growth rate m (eq. 1)
U	per genome mutation probability
N_0	initial number of wildtype individuals
m_0	wildtype growth rate
p_0	probability a wildtype individual has descendants that rescue the population
P	probability of rescue (eq. 2)
$p(m, \Lambda(m))$	probability a genotype with growth rate m , it-self fated for extinction, has descendants that rescue the population (eq. 3)
$p_{est}(m)$	probability a genotype with growth rate m establishes, i.e., rescues the population (eq. 4)
$\Lambda(m)$	probability that an individual with growth rate m produces a mutant that has descendants that rescue the population
$\Lambda_i(m)$	probability that an individual with growth rate m produces a mutant that has descendants with $i - 1$ additional mutations that rescue the population
$\Lambda_2^i(m)$	probability that an individual with growth rate m produces sufficiently subcritical ($i = " - "$), critical ($i = 0$), or supercritical ($i = " + "$) first-step mutants that eventually lead to 2-step rescue (eq. 8)
ψ	$2(1 - \sqrt{1 - m/m_{max}})$
ψ_0	$2(1 - \sqrt{1 - m_0/m_{max}})$
ρ_{max}	m_{max}/λ
α	$\rho_{max} \psi_0^2 / 4$

Table 1 Frequently used notation.

491 Taking the first order approximation of $p(m_0, \Lambda_1(m_0))$ with
 492 $\Lambda_1(m_0)/m_0^2$ small gives the probability of 1-step rescue (equation
 493 5 of [Anciaux et al. 2018](#)), which effectively assumes deter-
 494 ministic wildtype decline. For completeness we rederive their
 495 closed-form approximation in File S1 (and give the results in the
 496 Appendix, see [Approximating the probability of 1-step rescue](#)).

497 The probability of 2-step rescue is only slightly more compli-
 498 cated. Here $\Lambda_2(m_0)$ is the probability that a mutation arising on
 499 the wildtype background creates a genotype that is also fated
 500 for extinction but persists long enough for a second mutation
 501 to arise on this mutant background, creating a double mutant
 502 genotype that rescues the population. We therefore have

$$\Lambda_2(m_0) = U \int_{-\infty}^{m_{\max}} f(m|m_0) [1 - p_{\text{est}}(m)] p(m, \Lambda_1(m)) dm. \quad (6)$$

Following this logic, we can retrieve the probability of k -step rescue, for arbitrary $k \geq 2$, using the recursion

$$\Lambda_k(m_0) = U \int_{-\infty}^{m_{\max}} f(m|m_0) [1 - p_{\text{est}}(m)] p(m, \Lambda_{k-1}(m)) dm, \quad (7)$$

with the initial condition given by Equation 5.

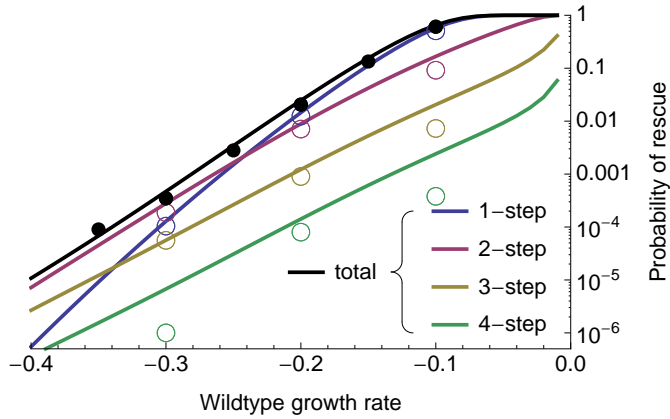


Figure 3 The probability of evolutionary rescue as a function of initial maladaptation. Shown are the probabilities of 1-, 2-, 3-, and 4-step rescue (using Equations 2-7), as well as the probability of rescue by up to 4 mutational steps ("total", using $\Lambda(m_0) = \sum_{i=1}^4 \Lambda_i(m_0)$). Circles are individual-based simulation results (ranging from 10^5 to 10^6 replicates per wildtype growth rate). Open circles denote the fraction of simulations where the rescue genotype (see [Simulation procedure](#)) had a given number of mutations and closed circles are the sum of these fractions. Parameters: $N_0 = 10^4$, $U = 2 \times 10^{-3}$, $n = 4$, $\lambda = 0.005$, $m_{\max} = 0.5$.

506 Approximating the probability of 2-step rescue

The probability of 2-step rescue is given by Equation 2 with $p_0 = p(m_0, \Lambda_2(m_0))$ (Equations 3-6). We next develop some intuition by approximating this for different classes of single mutants.

First, note that when the growth rate of a first-step mutation is close enough to zero such that $m^2 \ll \Lambda_1(m)$, we can approximate the probability that such a genotype leads to rescue before itself going extinct, $p(m, \Lambda_1(m))$, using a Taylor series, as $\sqrt{2\Lambda_1(m)}$ (c.f. equation A.4b in [Iwasa et al. 2004a](#), see also File S1). We can also derive this result heuristically by considering the probability that a lineage will persist long enough that it will incur a secondary rescue mutation. As shown in the Appendix (see [Mutant lineage dynamics](#)), while $t < 1/|m|$ a mutant lineage with growth rate m that is destined for extinction persists for t generations with probability $\sim 2/t$ (Equation 21) and in generation t since it has arisen has $\sim t/2$ individuals (Equation 22). Thus, while $T < 1/|m|$ a mutant lineage that persists for T generations will have produced a cumulative number $\sim T^2/4$ individuals. Such lineages will then lead to 2-step rescue with probability $\sim \Lambda_1(m)T^2/4$ until this approaches 1,

527 near $T = 2/\sqrt{\Lambda_1(m)}$. Since the probability of rescue increases
 528 like T^2 while the probability of persisting to time T declines only
 529 like $1/T$, most rescue events will be the result of rare long-lived
 530 single mutant genotypes. Considering only the most long-lived
 531 genotypes, the probability that a first-step mutation leads to
 532 rescue is then the probability that it survives long enough to
 533 almost surely rescue, i.e., for $T \sim 2/\sqrt{\Lambda_1(m)}$ generations. Since
 534 the probability of such a long-lived lineage is $2/T \sim \sqrt{\Lambda_1(m)}$,
 535 this heuristic result agrees with our Taylor series approximation
 536 of Equation 5. Thus, for first-step mutants with growth rates
 537 satisfying $2/\sqrt{\Lambda_1(m)} < 1/|m|$, implying $m^2 \ll \Lambda_1(m)$, which
 538 occur with probability $\sim \sqrt{\Lambda_1(m)}$, persistence is long enough
 539 to almost certainly ensure rescue. This same reasoning has been
 540 used to explain why the probability that a neutral mutation seg-
 541 regates long enough to produce a second mutation is $\sim \sqrt{U}$ in a
 542 population of constant size ([Weissman et al. 2009](#)).

543 At the other extreme, when the growth rate of a first-step
 544 mutation is far enough from zero such that $m^2 \gg \Lambda_1(m)$, we
 545 can approximate $p(m, \Lambda_1(m))$, again using a Taylor series, with
 546 $\Lambda_1(m)/|m|$ (c.f. equation A.4c in [Iwasa et al. 2004a](#), see also File
 547 S1). Conditioned on extinction such genotypes cannot persist
 548 long enough to almost surely lead to 2-step rescue. Instead, we
 549 expect such mutations to persist for at most $\sim 1/|m|$ genera-
 550 tions (Equation 21) with a lineage size of ~ 1 individual per
 551 generation (Equation 22), and thus produce a cumulative total
 552 of $\sim 1/|m|$ individuals. The probability of 2-step rescue from
 553 such a first-step mutation is therefore $\Lambda_1(m)/|m|$, and again this
 554 heuristic argument matches our Taylor series approach. This
 555 same reasoning explains why a rare mutant genotype with selec-
 556 tion coefficient $|s| \gg 0$ in a constant population size model is
 557 expected to have a cumulative number of $\sim 1/|s|$ descendants,
 558 given it eventually goes extinct ([Weissman et al. 2009](#)).

559 The transitions between these two regimes occur when
 560 $\Lambda_1(m)/|m| = \sqrt{2\Lambda_1(m)}$, i.e., when $|m| = \sqrt{\Lambda_1(m)/2}$. We
 561 call single mutants with growth rates $m < -\sqrt{\Lambda_1(m)/2}$ "suf-
 562 ficiently subcritical", those with $|m| < \sqrt{\Lambda_1(m)/2}$ "sufficiently
 563 critical", and those with $m > \sqrt{\Lambda_1(m)/2}$ "sufficiently supercrit-
 564 ical". Given that U and thus $\Lambda_1(m)$ will generally be small, m
 565 will also be small at these transition points, meaning we can
 566 approximate the transition points as $m^* = \sqrt{\Lambda_1(0)/2}$ and $-m^*$.
 567 We then have an approximation for the rate of 2-step rescue,

$$\begin{aligned} \Lambda_2(m_0) &= \Lambda_2^{(-)}(m_0) + \Lambda_2^{(0)}(m_0) + \Lambda_2^{(+)}(m_0) \\ \Lambda_2^{(-)}(m_0) &= U \int_{-\infty}^{-m^*} f(m|m_0) \Lambda_1(m)/|m| dm \\ \Lambda_2^{(0)}(m_0) &= U \int_{-m^*}^{m^*} f(m|m_0) [1 - p_{\text{est}}(m)] \sqrt{2\Lambda_1(m)} dm \\ \Lambda_2^{(+)}(m_0) &= U \int_{m^*}^{m_{\max}} f(m|m_0) [1 - p_{\text{est}}(m)] \Lambda_1(m)/|m| dm \end{aligned} \quad (8)$$

568 where $\Lambda_2^{(i)}(m_0)$ is the rate of 2-step rescue through suffi-
 569 ciently subcritical first-step mutants ($i = " - "$), suffi-
 570 ciently critical first-step mutants ($i = 0$), or suffi-
 571 ciently supercritical first-step mutants ($i = " + "$). A schematic depicting the 1- and 2-step
 572 genetic paths to rescue is given in Figure 4.

573 **Closed-form approximation for critical 2-step rescue** When U
 574 is small m^* is also small, allowing us to use $m = 0$ within the
 575 integrand of $\Lambda_2^{(0)}(m_0)$, which spans a range, $[-m^*, m^*]$, of width
 576 $2m^* \approx \sqrt{2\Lambda_1(0)}$, giving

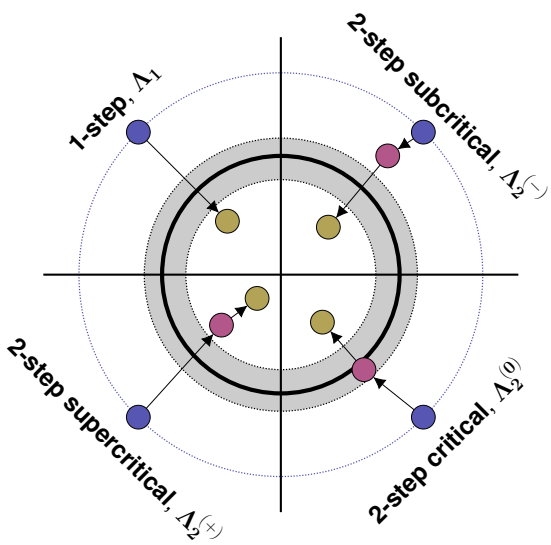


Figure 4 1- and 2-step genetic paths to evolutionary rescue. Here we show an $n = 2$ dimensional phenotypic landscape. Continuous-time (Malthusian) growth rate (m) declines quadratically from the centre, becoming negative outside the thick black line. The grey zone indicates where growth rates are “sufficiently critical” (see text for details). Blue circles show wildtype phenotypes, red circles show intermediate first-step mutations, and yellow circles show the phenotypes of rescue genotypes.

$$\begin{aligned} \Lambda_2^{(0)}(m_0) &\approx U f(0|m_0) \sqrt{2\Lambda_1(0)} 2m^* \\ &= 2U f(0|m_0) \Lambda_1(0). \end{aligned} \quad (9)$$

We can then approximate $\Lambda_1(m)$ with $\tilde{\Lambda}_1(m)$ (Equation 19) and take $m \rightarrow 0$ (Equation 20), giving a closed form approximation for the rate of 2-step rescue through critical single mutants in Fisher’s geometric model,

$$\Lambda_2^{(0)}(m_0) \approx 4U^2 f(0|m_0) \sqrt{m_{max}\lambda/\pi}. \quad (10)$$

This well approximates numerical integration of $\Lambda_2^{(0)}(m_0)$ (Equation 8; see Figure 5 and File S1). In general, it will perform better when the critical zone, and thus $U\sqrt{m_{max}\lambda}$, becomes smaller.

To get a better understanding of how the rate of 2-step critical rescue depends on the underlying parameters of Fisher’s geometric model, we approximate $f(m|m_0)$, assuming that the distance from the wildtype to the optimal phenotype is large relative to the distribution of mutations (i.e., $\rho_{max} = m_{max}/\lambda$ is large), and convert this to a distribution over $\psi = 2(1 - \sqrt{1 - m/m_{max}})$, a convenient rescaling (for details see File S1 and [Anciaux et al. 2018](#)). Evaluating this at $m = 0$ gives

$$\Lambda_2^{(0)}(m_0) \approx U^2 (1 - \psi_0/2)^{(1-n)/2} e^{-\alpha} \frac{2}{\pi}, \quad (11)$$

where $\psi_0 = 2(1 - \sqrt{1 - m_0/m_{max}}) < 0$ and $\alpha = \rho_{max}\psi_0^2/4$.

Closed-form approximations for non-critical 2-step rescue We can also approximate $\Lambda_1(m)$ in $\Lambda_2^{(-)}(m_0)$ and $\Lambda_2^{(+)}(m_0)$ with $\tilde{\Lambda}_1(m)$ (Equation 19), leaving us with just one integral over

the growth rates of the first-step mutations. We then replace $f(m|m_0)$ with its approximate distribution over ψ as above.

In the case of subcritical rescue we can then make two contrasting approximations (see File S1 for details). First, when the ψ (and thus m) that contribute most are close enough to zero (meaning maladaptation is not too large relative to mutational variance) and we ignore mutations that are less fit than the wildtype, we find the rate of subcritical 2-step rescue is roughly

$$\Lambda_2^{(-)}(m_0) \approx U^2 \frac{(1 - \psi_0/2)^{1-n}}{1 - \psi_0/4} e^{-\alpha} \frac{\log(\psi_0/\psi_-^*)}{\pi}, \quad (12)$$

where $\psi_-^* = 2(1 - \sqrt{1 + \tilde{m}^*/m_{max}}) < 0$ and $\tilde{m}^* = \sqrt{\tilde{\Lambda}_1(0)/2}$ (Equation 20). Second, when the mutational variance, λ , is very small relative to maladaptation, implying that mutants far from $m = 0$ substantially contribute, we find the rate of subcritical 2-step rescue to be nearly

$$\Lambda_2^{(-)}(m_0) \approx -U^2 \frac{(1 - \psi_0/2)^{1-n}}{1 - \psi_0/4} \left(e^{-\alpha} \frac{1}{(\alpha/2)^3 \pi} \right)^{1/2}. \quad (13)$$

These two approximations do well compared with numerical integration of $\Lambda_2^{(-)}(m_0)$ (Equation 8; see Figure 5 and File S1). As expected, we find that Equation 13 does better under fast wildtype decline while Equation 12 does better when the wildtype is declining more slowly.

For supercritical 2-step rescue, only first-step mutants with growth rates near m^* will contribute (larger m will rescue themselves and are also less likely to arise by mutation), and so we can capture the entire distribution with a small m approximation (following the same approach that led to Equation 12). As shown in File S1, this approximation works well for sufficiently small first-step mutant growth rates, $\psi < \sqrt{2/\rho_{max}}$, beyond which the rate of 2-step rescue through such first-step mutants falls off very quickly due to a lack of mutational input. Thus, considering only supercritical single mutants with scaled growth rate less than $\sqrt{2/\rho_{max}}$, our approximation is

$$\Lambda_2^{(+)}(m_0) \approx U^2 \frac{(1 - \psi_0/2)^{1-n}}{1 - \psi_0/4} e^{-\alpha} \frac{\log(\psi_{max}/\psi_+^*)}{\pi}, \quad (14)$$

with $\psi_+^* = 2(1 - \sqrt{1 - \tilde{m}^*/m_{max}})$ and $\psi_{max} = \sqrt{2/\rho_{max}}$. This approximation tends to provide a slight overestimate of $\Lambda_2^{(+)}(m_0)$ (Equation 8; see Figure 5 and File S1).

Comparing 2-step regimes These rough but simple closed-form approximations (Equations 11–14) show that, while the contribution of critical mutants to 2-step rescue scales with U^2 , the contribution of non-critical single mutants scales at a rate less than U^2 (Figure 5B) due to a decrease in ψ_-^* (decreasing the range of subcritical mutants) and an increase in ψ_+^* (decreasing the range of supercritical mutants) with U . This difference in scaling with U is stronger when the wildtype is not very maladapted relative to the mutational variance, i.e., when Equation 12 is the better approximation for subcritical rescue. The approximations also show that when initial maladaptation is small, the ratio of supercritical to subcritical contributions (Equation 12 divided by 14) primarily depends on the range of growth rates included in each regime, while with larger initial maladaptation this ratio (Equation 13 divided by 14) begins to depend more strongly on initial maladaptation and mutational variance (α). The effect of maladaptation and mutation rate on the relative contributions of each regime is shown in Figure 5.

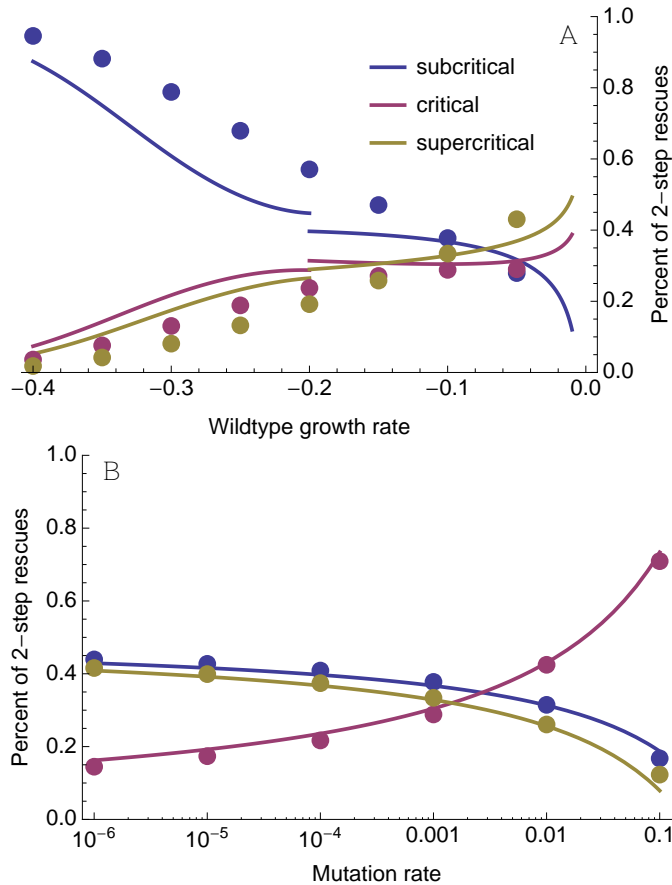


Figure 5 The relative contribution of sufficiently subcritical, critical, and supercritical single mutants to 2-step rescue. The curves are drawn using Equations 10–14 (Equation 12 is used for $m_0 < 0.2$ while Equation 13 is used for $m_0 > 0.2$). The dots are numerical evaluations of Equation 8. Parameters: $n = 4$, $\lambda = 0.005$, $m_{max} = 0.5$, (A) $U = 10^{-3}$, (B) $m_0 = -0.1$.

646 The distribution of growth rates among rescue genotypes

647 We next explore the distribution of growth rates among rescue
 648 genotypes, i.e., the distribution of growth rates that we expect
 649 to observe among the survivors across many replicates.

650 We begin with 1-step rescue. The rate of 1-step rescue by
 651 genotypes with growth rate m is simply $Uf(m|m_0)p_{est}(m)$. Di-
 652 viding this by the rate of 1-step rescue through any m (Equation
 653 5) gives the distribution of growth rates among the survivors

$$654 g_1(m) = \frac{Uf(m|m_0)p_{est}(m)}{\Lambda_1(m_0)}, \quad (15)$$

655 where the mutation rate, U , cancels out. This distribution is
 656 shown in blue in Figure 6. The distribution has a mode at small
 657 but positive m as a result of two conflicting processes: smaller
 658 growth rates are more likely to arise from a declining wildtype
 659 but larger growth rates are more likely to establish given they
 660 arise. As the rate of wildtype decline increases, the former pro-
 661 cess exerts more influence, causing the mode to move towards
 662 zero and reducing the variance.

663 We can also give a simple, nearly closed-form approximation
 664 here using the same approach taken to reach Equation 19. On the
 665 ψ scale, the distribution of effects among 1-step rescue mutations
 666 is

$$666 \tilde{g}_1(\psi) = \frac{\exp(\alpha)\sqrt{\alpha\rho_{max}}}{[\exp(\alpha)\sqrt{\pi\alpha}\text{Erfc}(\sqrt{\alpha}) - 1]\psi_0} e^{-\rho_{max}(\psi-\psi_0)^2/4}\psi, \quad (16)$$

667 implying the ψ are distributed like a normal truncated below
 668 $\psi = 0$ and weighted by ψ . This often provides a very good
 669 approximation (see dashed blue curves in Figure 6).

670 In 2-step rescue, the rate of rescue by double mutants with
 671 growth rate m_2 is given by Equation 6 with $\Lambda_1(m)$ replaced
 672 by $Uf(m_2|m)p_{est}(m_2)$. Normalizing gives the distribution of
 673 growth rates among the double mutant genotypes that rescue the
 674 population

$$674 g_2(m_2) \approx \frac{A(m_2)}{\int_0^{m_{max}} A(m_2)dm_2} \quad (17)$$

$$675 A(m_2) = \int_{-\infty}^{m_{max}} f(m|m_0) [1 - p_{est}(m)]$$

$$676 p(m, Uf(m_2|m)p_{est}(m_2))dm.$$

677 This distribution, $g_2(m)$, is shown in red in Figure 6. Because the
 678 first-step mutants contributing to 2-step rescue tend to be nearer
 679 the optimum than the wildtype, this allows them to produce
 680 double mutant rescue genotypes with higher growth rates than
 681 in 1-step rescue (as seen by comparing the mode between blue
 682 and red curves in Figure 6). The fact that these first-step mutants
 683 are closer to the optimum also allows for a greater variance in the
 684 growth rates of rescue genotypes than in 1-step rescue. Thus the
 685 2-step distribution maintains a more similar mode and variance
 686 across wildtype decline rates than the 1-step distribution. Note
 687 that because $g_2(m_2)$ depends on U the buffering effect of first-
 688 step mutants depends on the mutation rate (see [The distribution of growth rates among rescue intermediates](#) below for more
 689 discussion).

688 The distribution of growth rates among rescue intermediates

689 Finally, our analyses above readily allow us to explore the distribution
 690 of first-step mutant growth rates that contribute to 2-step
 691 rescue. Analogously to Equation 15, we drop the integral in
 692 $\Lambda_2(m_0)$ (Equation 6) and normalize, giving

$$693 h(m) = \frac{Uf(m|m_0) [1 - p_{est}(m)] p(m, \Lambda_1(m))}{\Lambda_2(m_0)}, \quad (18)$$

694 where the first U cancels but the U within $\Lambda_1(m)$ does not. This
 695 distribution is shown in black in Figure 7. At slow wildtype
 696 decline rates the overwhelming majority of 2-step rescue events
 697 arise from first-step mutants with growth rates near 0. As in-
 698 dicated by Equation 8, the contribution of first-step mutants
 699 with growth rate m declines as $\sim 1/|m|$ as m departs from zero,
 700 due to shorter persistence times given eventual extinction. As
 701 wildtype growth rate declines, the relative importance of muta-
 702 tional input, $f(m|m_0)$, grows, causing the distribution to flatten
 703 and first-step mutants with substantially negative growth rates
 704 begin to contribute (compare panels in Figure 7; see also Figure
 705 5A). Decreasing the mutation rate disproportionately increases
 706 the contribution of first-step mutants with growth rates near
 707 zero (while simultaneously shrinking the range of growth rates
 708 that are sufficiently critical; Figure 5B) making the distribution
 709 of first-step mutant growth rates contributing to 2-step rescue
 710 more sharply peaked around $m = 0$ (Figure S2). Correspond-
 711 ingly, with a higher mutation rate a greater proportion of the
 712 contributing single mutants have substantially negative growth
 713 rates.

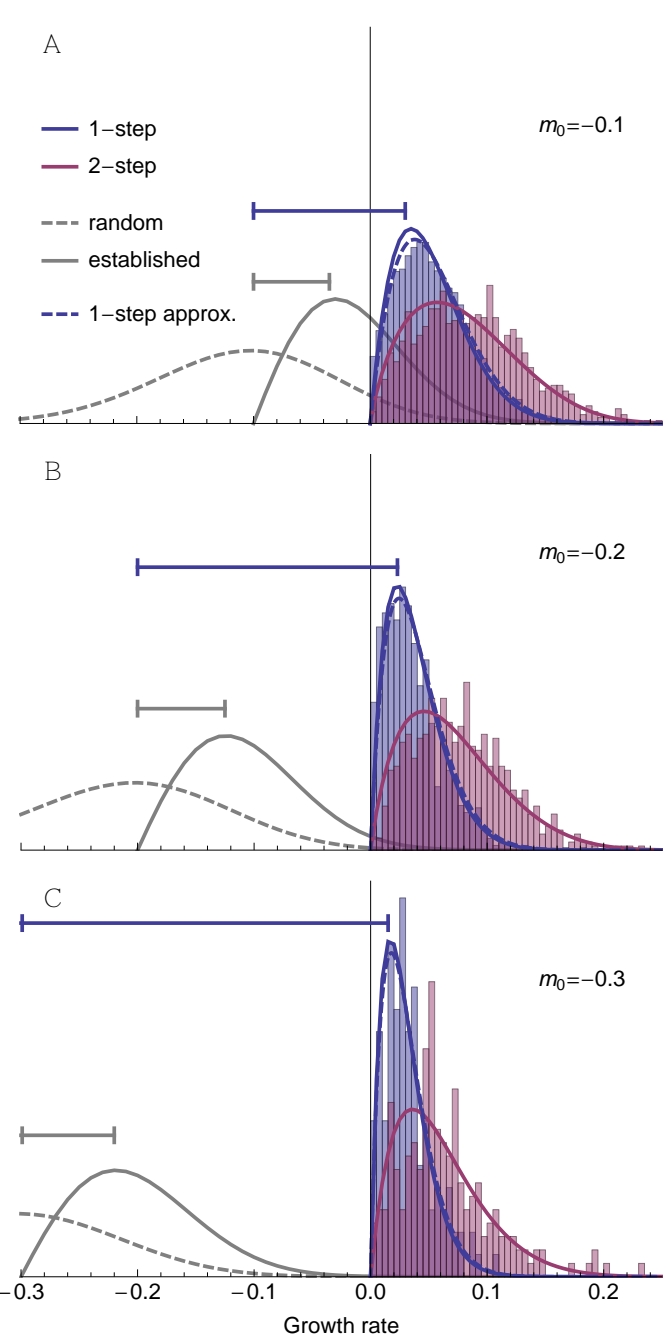


Figure 6 The distribution of growth rates among rescue genotypes under 1-step (blue; Equation 15 solid and 16 dashed) and 2-step (red; Equation 17) rescue for three different levels of initial maladaptation. For comparison, the distribution of random mutations (dashed; Equation 1) and the distribution of beneficial mutations that establish in a population of constant size (solid grey; Equation 1 times Equation 4 and normalized) are shown. Intervals (horizontal lines) indicate the size of the most common fitness effect ($s = m_0 - m$) in a population of constant size (grey) and in 1-step rescue (blue). The histograms show the distribution of growth rates among rescue genotypes observed across (A) 10^4 , (B) 10^5 , and (C) 10^6 simulated replicates. Other parameters: $N_0 = 10^4$, $U = 2 \times 10^{-3}$, $n = 4$, $\lambda = 0.005$, $m_{max} = 0.5$.

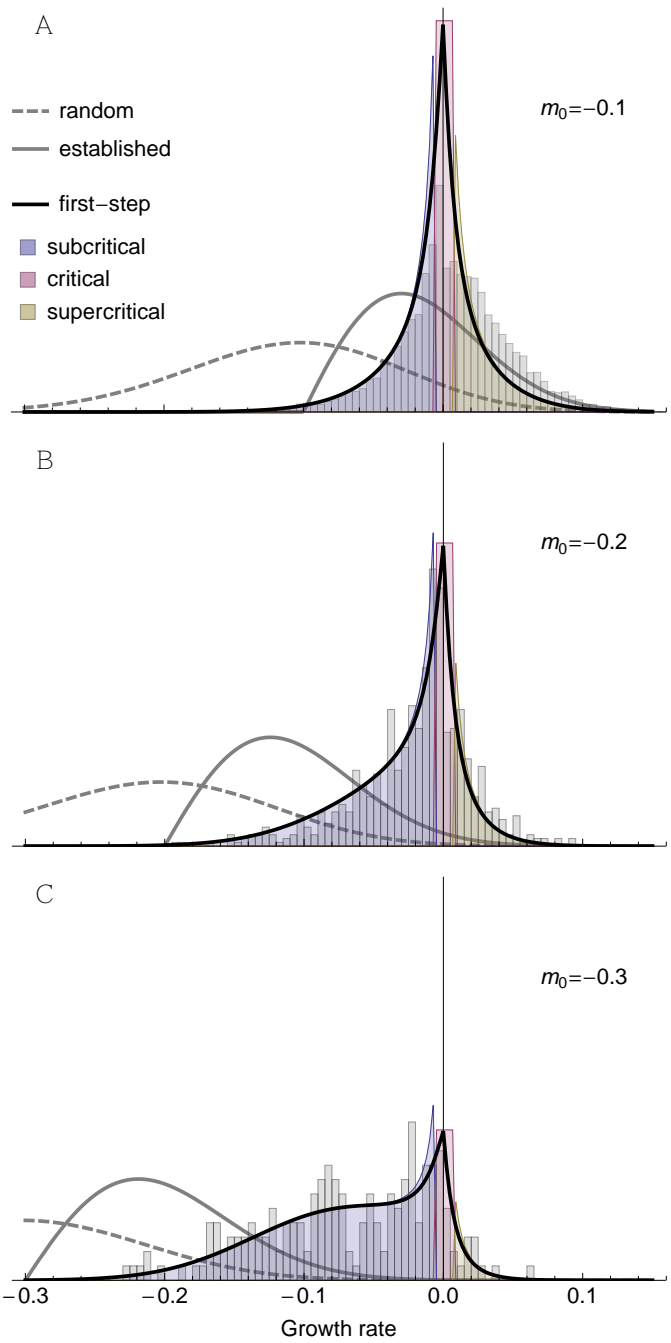


Figure 7 The distribution of growth rates among first-step mutations that lead to 2-step rescue (black; Equation 18) for three different levels of initial maladaptation. Shading represents our sufficiently subcritical approximation (blue; replacing $p(m, \Lambda_1(m))$ with $\Lambda_1(m)/|m|$ in the numerator of Equation 18), our sufficiently critical approximation (red; using $Uf(0|m_0|)\sqrt{2\Lambda_1(0)}$ as the numerator in Equation 18), and our sufficiently supercritical approximation (yellow; replacing $p(m, \Lambda_1(m))$ with $\Lambda_1(m)/|m|$ in the numerator of Equation 18). The histograms show the distribution of growth rates among first-step mutations in rescue genotypes with 2 mutations observed across (A, B) 10^5 or (C) 10^6 simulated replicates. We hypothesize that the overabundance of supercriticals (especially in panel A) is likely due to us sampling only the most common rescue genotype in each replicate, which is not necessarily the first genotype that rescues. See Figure 6 for additional details.

713 Discussion

714 Here we have explored the probability and genetic basis of evolutionary rescue by multiple mutations on a simple fitness landscape. We find that rescue by multiple mutations can be the 715 most likely path to persistence under high mutation rates or 716 when the population is initially very maladapted. Under these 717 scenarios, intermediate genotypes that are declining less quickly 718 provide a 'springboard' from which rescue genotypes emerge. In 719 2-step rescue these springboard single mutants come from one 720 of three regimes: those that have growth rates near enough to 721 zero ("sufficiently critical") that rescue is most likely when a 722 mutation persists for an unusually long period of time and grows to 723 an unusually large subpopulation size, and those with growth 724 rates that are either negative or positive enough ("sufficiently 725 subcritical" or "sufficiently supercritical", respectively) to restrict 726 persistence times and subpopulation sizes, conditioned upon 727 the loss of the first mutation in the absence of a second, rescuing 728 mutation. The relative contribution of each regime shifts with 729 initial maladaptation and mutation rate; rare mutations that can 730 occasionally reach unusually large subpopulation sizes play a 731 larger role when the population is not severely maladapted (e.g., 732 Figure 7A) or mutation rate is high (e.g., Figure S2C). In contrast, 733 when populations are initially very maladapted (e.g., Figure 7C), 734 most first-step mutations are themselves also very maladapted 735 and thus restricted in the subpopulation sizes they are expected 736 to reach before being lost. All three regimes help to maintain the 737 variance in the distribution of fitness effects among rescue 738 genotypes as initial maladaptation increases; meanwhile, in 1-step 739 rescue the variance declines due to ever more extreme sampling 740 of the tail of the mutational distribution (compare blue and red 741 curves in Figure 6).

742 Our prediction, that rescue by more *de novo* mutations can be 743 more likely than rescue by fewer, is novel. In previous models 744 (e.g., Antia *et al.* 2003; Iwasa *et al.* 2004a; Alexander and Day 745 2010) the general conclusion has been that, since the probability 746 of rescue scales with U^k (where U is the mutation rate and k 747 is the minimum number of mutations required for rescue), the 748 probability of rescue declines with the number of mutations. 749 This assumes, however, that the probability of a mutation occurring, 750 U , is the limiting factor. Here we have shown that when 751 the probability of a beneficial mutation arising declines with its 752 selective advantage, the probability of sampling once from the 753 extreme tail of the DFE can be lower than sampling multiple 754 mutations closer to the bulk of the DFE, so that rescue via multiple 755 mutations can become the dominant path. Rescue by multiple 756 mutations may also be more likely with standing genetic variation, 757 as small-effect intermediate mutations may segregate at 758 higher frequencies than large-effect rescue mutations before the 759 environmental change (and also decline less quickly than the 760 wildtype following environmental change); this is especially 761 true with recombination, where rescue genotypes can arise from 762 segregating intermediate mutations without mutation (Uecker 763 and Hermisson 2016).

764 How often rescue arises as a result of multiple mutations is 765 an open question. It is clear that more than one mutation can 766 contribute to adaptation to near-lethal stress, but experiments 767 are often designed to avoid extinction (reviewed in Cowen *et al.* 768 2002) and therefore greatly expand the scope for multiple 769 mutations to arise on a single genotype. A few exceptions provide 770 some insight. For example, populations of *Saccharomyces cerevisiae* 771 that survived high concentrations of copper acquired multiple 772 mutations (Gerstein *et al.* 2015) – in fact the authors argue for 773

774 the 'springboard effect' discussed above, where first-step mutations 775 prolong persistence and thereby allow further mutations to 776 arise. In *Pseudomonas fluorescens*, fluctuation tests with nalidixic 777 acid showed that nearly a third of the most resistant surviving 778 strains were double mutants (Bataillon *et al.* 2011), which were 779 able to tolerate 10x higher drug concentrations than single 780 mutants, suggesting 2-step rescue might dominate at high drug 781 concentrations. While suggestive, it is unclear if our prediction – 782 that rescue takes more mutational steps with greater initial 783 maladaptation – holds true generally. Verification will require more 784 experiments that allow extinction and uncover the genetic basis 785 of adaptation at different severities of environmental change 786 (e.g., drug concentration).

787 In describing the genetic basis of adaptation in populations 788 of constant size, Orr (1998) showed that the mean phenotypic 789 displacement towards the optimum scales roughly linearly with 790 initial displacement. Converting phenotype to fitness, this implies 791 that the mean fitness effect of fixed mutations ($s = m - m_0$) 792 increases exponentially as initial Malthusian fitness (m_0) declines 793 (i.e., $s \sim \exp(-m_0)$), which is a roughly linear increase when initial 794 fitness is small ($|m_0| \ll 1$). Here we see that, under 1-step 795 rescue, the mean fitness effect also increases roughly linearly as 796 the initial growth rate declines (see horizontal blue lines in Figure 797 6). However, the rate of this linear increase in fitness effect 798 is much larger under rescue than in a population of constant 799 size (compare blue and grey horizontal lines in Figure 6), where 800 declines in wildtype fitness not only allow larger mutations to be 801 beneficial but also require larger mutations for persistence. Thus 802 the race between extinction and adaptation during evolutionary 803 rescue is expected to produce a genetic basis of adaptation with 804 fewer mutations of larger effect.

805 While under 1-step rescue the fitness effect of the first mutation 806 increases roughly linearly as wildtype fitness declines, most 807 rescue events will be 2-step for wildtype fitnesses below some 808 value (e.g., at $m_0 \approx -0.25$ in Figure 3; this threshold value of 809 m_0 increases with mutation rate, Figure S1). At this junction 810 the effect size of the first mutation will no longer increase as 811 quickly (and potentially even decrease), as it switches from a 812 rescue mutant to an intermediate mutant whose expected fitness 813 begins to decline substantially with the fitness of the wildtype 814 (Figure 7). Thus as rescue switches from dominantly k -step to 815 dominantly $(k+1)$ -step the genetic basis of adaptation becomes 816 more diffuse, with each mutation having a smaller individual 817 fitness effect as the contributing fitness effects spread over more 818 loci. In the limit of large k (due to large initial maladaptation or 819 high mutation rates), the genetic basis of adaptation should at 820 some point converge to many loci with small effect, as would 821 also be expected in a population of constant size. Indeed, at 822 very high mutation rates the rate of adaptation (the change in 823 mean fitness) is the same under rescue as it is in populations 824 of constant size (Anciaux *et al.* 2019), implying that the genetic 825 basis of adaptation no longer depends on demography. It is 826 therefore at intermediate levels of initial maladaptation and low 827 mutation rates, where rescue primarily occurs from a few large 828 effect mutations, that the race between adaptation and persistence 829 is predicted to have the largest effect on the genetic basis 830 of adaptation.

831 Fluctuation tests (Luria and Delbrück 1943) provide a means 832 to generate random mutations and then isolate potential rescue 833 genotypes (typically assumed to be 1-step only), whose growth 834 rates can be measured under the selective conditions. These 835 experiments are designed such that there is substantial standing 836

genetic variation at the time of exposure to the selective conditions, which should increase the contributions of mutations with small growth rates (Orr and Betancourt 2001), although these could be outcompeted by mutations with higher growth rates and/or be under-sampled. Regardless, consistent with our theory (Figure 6), the resulting growth rate distributions in both bacteria and yeast often find modes that are substantially greater than zero (as opposed to, say, an exponential distribution; Kassen and Bataillon 2006; MacLean and Buckling 2009; Gerstein *et al.* 2012; Lindsey *et al.* 2013; Gerstein *et al.* 2015). A number of these conform even more closely to our expected shape (Kassen and Bataillon 2006; Gerstein *et al.* 2015) while the others appear to be substantially more clumped around the mode, perhaps due to a very restricted number of possible rescue mutations in any one circumstance, the size of the experiment, or the way in which growth rates are measured. Finally, Gerstein *et al.* (2015) not only provide the distribution of growth rates among rescue genotypes, but also the growth rates of individual mutations that compose multi-step rescue genotypes. In four lines where multiple mutations were detected and a segregation analysis performed, one mutation in each line was inferred to have a minor effect and the other mutation was an amplification of the copper metallothionein CUP with a major fitness effect. These results are consistent with the minor effect mutations being sub-critical mutations that provided a springboard for the larger CUP mutations.

Pinpointing the mutations responsible for adaptation is hampered by genetic hitchhiking, as beneficial alleles elevate the frequency of linked neutral and mildly deleterious alleles (Barton 2000). The problem is particularly severe under strong selection and low recombination, and therefore reaches an extreme in the case of evolutionary rescue in asexuals, especially if many neutral and deleterious mutations are segregating at the time of environmental change. To circumvent this, mutations that have risen to high frequency in multiple replicates are often introduced in a wildtype background, in isolation and sometimes also in combination with a small number of other common high-frequency mutations, and grown under the selective conditions (e.g., Jochumsen *et al.* 2016; Ono *et al.* 2017). As we have demonstrated above (e.g., Figure 7C), however, under multi-step rescue there may be no one mutation that individually confers growth in the selective conditions. Thus, a mutation that was essential for rescue may go undetected or be mistaken as a hitchhiker if the appropriate multiple-mutation genotypes are not tested. Unfortunately reverse engineering all combinations of mutations quickly becomes unwieldy as the number of mutations grows, and thus this approach will not be practical under severe initial maladaptation and high mutation rates, where we predict rescue to occur by many mutations. Interestingly, our simulations show that the population dynamics themselves may help differentiate how many mutations contribute to rescue (e.g., V- vs. U-shaped log-trajectories; Figures 1 and 2), and fitting models of k -step rescue could produce estimates for the growth rates of the k genotypes.

Environmental change often selects for mutator alleles, which elevate the rate at which beneficial alleles arise and subsequently increase in frequency with them (Tenaillon *et al.* 2001). When beneficial alleles are required for persistence, as in evolutionary rescue, mutator alleles can reach very high frequencies or rapidly fix (e.g., Mao *et al.* 1997). Consistent with this, mutator alleles are often associated with antibiotic resistance in clinical isolates (see examples in Bell 2017). Further, the more benefi-

cial mutations available the larger the advantage of a mutator allele; for a mutator that increases the mutation rate m -fold, its relative contribution to the production of n beneficial mutations scales as m^n (Tenaillon *et al.* 1999). Thus, conditions that cause multi-step rescue to be more likely than 1-step rescue should also impose stronger selection for mutator alleles. There are a number of examples where lineages with higher mutation rates acquired multiple mutations and persisted at higher doses of antibiotics (Couce *et al.* 2015; San Millan *et al.* 2017). The number of mutations required for persistence is, however, often unknown, making it difficult to compare situations where rescue requires different numbers of mutations. Experiments with a combination of drugs may provide a glimpse; for instance, *Escherichia coli* populations only evolved resistance to a combination of two drugs (presumably through the well-known mutations specific to each drug) when mutators were present, despite the fact that mutators were not required for resistance to either drug in isolation (Gifford *et al.* 2019). In cases where we have less information on the genetic basis of resistance, our model suggests that mutators will be more advantageous when initial maladaptation is severe (e.g., higher drug concentrations or a larger number of drugs), as rescue will then be dominated by genetic paths with more mutational steps.

Here we have investigated the genetic basis of evolutionary rescue in an asexual population that is initially genetically uniform. Extending this work to allow for recombination and standing genetic variation at the time of environmental change – as expected for many natural populations – would be valuable. The effect of standing genetic variation on the probability of 1-step rescue is relatively straight-forward to incorporate, depending only on the expected number of rescue mutations initially present and their mean establishment probability (Martin *et al.* 2013). In the case of the fluctuation tests discussed above, where mutations accumulated in the short interval before the onset of selection are assumed to be relatively neutral, the effect of standing genetic variance on 1-step rescue might be incorporated by a simple rescaling of N_0 , to account for the additional mutants present in the standing variation. When considering longer periods of time in populations that are not rapidly expanding, mutation-selection balance may be reached before the onset of selection. In this case the probability of 1-step rescue from standing genetic variance in Fisher's geometric model was given by Anciaux *et al.* (2018), whose equations 3 and 5 immediately give the distribution of fitness effects among those that rescue. Allowing these standing genetic variants to be springboards to multi-step rescue will help clarify the role of standing genetic variation on the genetic basis of rescue more generally. Recombination can help combine such springboard mutations into rescue genotypes but will also break these combinations apart, as demonstrated in a 2-locus 2-allele model of rescue (Uecker and Hermisson 2016). How recombination affects the genetic basis of evolutionary rescue when more loci can potentially contribute remains to be seen. Also left unexplored is the effect of density-dependent fitness; for example, competition may reduce mutant growth rates and thereby increase the size of mutations that are required for rescue, especially when the wildtype declines slowly. Combining density-dependence and standing genetic variance is known to create complex dynamics in a 1-locus 2-allele model of rescue (Uecker *et al.* 2014), and adding more potential genotypes is sure to add yet more complexity.

Many of our simple closed-form results rely upon knowing

961 the distribution of mutant growth rates (Equation 1), which 1023 arises from the assumption that mutant phenotypes are nor- 1024 mally distributed about their ancestor and Malthusian fitness 1025 is a quadratic, on some scaled phenotypic axes. It is clear that 1026 deviations from these assumptions will, at least quantitatively, 1027 affect our results. For instance, mutant phenotype distributions 1028 with truncated or fat tails are likely to lead to smaller or larger 1029 mutational steps, respectively, with downstream effects on the 1030 probability of rescue, the number of contributing mutations, and 1031 the resulting DFEs. As a preliminary investigation of this pre- 1032 diction, we have performed simulations with mutant phenotype 1033 distributions having the same expectation and covariances as 1034 assumed above under normality, but with truncated (platykurtic) 1035 or fat (leptokurtic) tails (Figure S3A). While our qualitative 1036 results above hold, the probability of rescue declines slower with 1037 wildtype maladaptation when the mutational distribution has 1038 fatter tails (compare dotted and solid black in Figure S3C). Fatter 1039 tails also reduce the number of mutations contributing to rescue 1040 (e.g., 1-step rescue dominates for all wildtype decline rates in 1041 Figure S3C). Finally, fatter tails cause the distributions of rescue 1042 genotype growth rates following 1- and 2-step rescue to have 1043 more variance and become more similar to one another (Figure 1044 S4B) and also tend to increase the contribution of supercritical 1045 single mutants in 2-step rescue (Figure S5). All told, the genetic 1046 basis of rescue is expected to consist of fewer mutations of larger 1047 effect, with less consistent effect sizes across replicate popula- 1048 tions, as the tails of the mutant phenotype distribution become 1049 fatter.

989 In the numerical examples above we have not varied the 1049 number of scaled phenotypic axes, n , i.e., the dimensionality of 1050 the phenotypic landscape (although the analytical results apply 1051 for arbitrary n). Because increasing the number of dimensions 1052 changes the distribution of fitness effects, and in particular de- 1053 creases the proportion of mutations that are beneficial (Fisher 1054 1930), this may have cascading influences on our results. As 1055 shown in Anciaux *et al.* (2018), the probability of 1-step rescue 1056 by *de novo* mutation declines with dimensionality, and is only 1057 weakly dependent on dimensionality when initial maladaptation 1058 is small (such that $\Lambda_1(m_0) \approx -m_0 U g(\alpha)$, Equation 19). 1059 Here we show that the distribution of fitness effects among 1- 1060 step rescue mutants is nearly independent of dimensionality for 1061 any degree of initial maladaptation (Equation 16 and the blue 1062 curves in Figure S6B). Further, as seen by comparing Equations 1063 11-14 to Equation 19, the probability of 2-step rescue depends 1064 on dimensionality much like 1-step rescue does, suggesting that 1065 while increasing dimensionality may decrease the probability 1066 of rescue it may have little effect on the number of steps rescue 1067 tends to take. This is demonstrated more generally in Figure 1068 S6A, where an order of magnitude increase in the number of 1069 dimensions decreases the probability of rescue by roughly an 1070 order of magnitude but has little effect on the relative rates of 1-, 1071 2-, 3-, and 4-step rescue. Finally, Figure S6B-C shows that dimen- 1072 sionality has very little effect on the distribution of fitness effects 1073 among 2-step rescue genotypes (Equation 17) and among first 1074 step mutants leading to 2-step rescue (Equation 18). To conclude, 1075 while the probability of rescue declines with the complexity of 1076 the organism and its environment, the genetic basis of rescue is 1077 expected to be relatively invariant across complexity, as with the 1078 genetic basis of adaptation in populations of constant size (Orr 1079 1998, see also gray curves in Figure S6B,C).

1021 In the numerical examples above we have also focused on a 1080 particular value of mutational variance, λ . Clearly, since rescue 1081

relies on mutations of large effect, decreasing λ should decrease the probability of rescue, much like decreasing the mutation rate, U , does (Figure S1). While our analysis (Equations 19 and 11-14) and numerical results (see File S1) show that this is true, we find that λ and U have very different effects on the genetic basis of rescue (File S1). In particular, given a similar effect on the total probability of rescue, decreasing U generally restricts rescue to fewer mutational steps while decreasing λ forces rescue to occur by more mutations. Further, the distribution of fitness effects of mutations contributing to rescue is nearly independent of U but a decrease in λ strongly reduces the mode of the DFE. This demonstrates that populations with similar probabilities of rescue can vary greatly in the way they achieve it genetically.

Acknowledgements

We would like to thank the Otto and Doebeli labs for helpful feedback at various stages, Ophélie Ronce and Thomas Lenormand for their hospitality and valuable input at the beginning of this project, and Mike Whitlock, Amy Angert, Luis-Miguel Chevin, and Joachim Hermisson for constructive criticism on previous versions of the manuscript. Funding provided by the National Science and Engineering Research Council (CGS-D 6564 to M.M.O., RGPIN-2016-03711 to S.P.O.), the University of British Columbia, Banting, and the University of California - Davis (fellowships to M.M.O.), the National Institute of General Medical Sciences of the National Institutes of Health (NIH R01 GM108779 to Graham Coop), the Agence Nationale de la Recherche (ANR-18-CE45-0019 "RESISTE" to G.M.), and the Centre Méditerranéen Environnement et Biodiversité ("BACTPHI" to G.M.).

Literature Cited

Abramowitz, M. and I. A. Stegun, editors, 1972 *Handbook of mathematical functions with formulas, graphs, and mathematical tables*. United States Department of Commerce, Washington, DC, USA.

Alexander, H. K. and T. Day, 2010 Risk factors for the evolutionary emergence of pathogens. *Journal of the Royal Society Interface* 7: 1455–1474.

Alexander, H. K., G. Martin, O. Y. Martin, and S. Bonhoeffer, 2014 Evolutionary rescue: linking theory for conservation and medicine. *Evolutionary Applications* 7: 1161–1179.

Allen, L. J., 2010 *An introduction to stochastic processes with applications to biology*. CRC Press.

Anciaux, Y., L.-M. Chevin, O. Ronce, and G. Martin, 2018 Evolutionary rescue over a fitness landscape. *Genetics* 209: 265–279.

Anciaux, Y., A. Lambert, O. Ronce, L. Roques, and G. Martin, 2019 Population persistence under high mutation rate: from evolutionary rescue to lethal mutagenesis. *Evolution*.

Antia, R., R. R. Regoes, J. C. Koella, and C. T. Bergstrom, 2003 The role of evolution in the emergence of infectious diseases. *Nature* 426: 658.

Barton, N. H., 2000 Genetic hitchhiking. *Philosophical Transactions of the Royal Society of London. Series B: Biological Sciences* 355: 1553–1562.

Bataillon, T. and S. F. Bailey, 2014 Effects of new mutations on fitness: Insights from models and data. *Annals of the New York Academy of Sciences* 1320: 76–92.

Bataillon, T., T. Zhang, and R. Kassen, 2011 Cost of adaptation and fitness effects of beneficial mutations in *pseudomonas fluorescens*. *Genetics* 189: 939–949.

1082 Bell, G., 2009 The oligogenic view of adaptation. *Cold Spring 1144*
1083 Harbor Symposia on Quantitative Biology **74**: 139–144. 1145

1084 Bell, G., 2017 Evolutionary rescue. *Annual Review of Ecology, 1146*
1085 Evolution, and Systematics **48**: 605–627. 1147

1086 Couce, A., A. Rodríguez-Rojas, and J. Blázquez, 2015 Bypass 1148
1087 of genetic constraints during mutator evolution to antibiotic 1149
1088 resistance. *Proceedings of the Royal Society B: Biological Sci- 1150*
1089 ences **282**: 20142698. 1151

1090 Cowen, L. E., J. B. Anderson, and L. M. Kohn, 2002 Evolution 1152
1091 of drug resistance in *candida albicans*. *Annual Reviews in 1153*
1092 Microbiology

1093 **56**: 139–165. 1154

1094 Dettman, J. R., N. Rodrigue, A. H. Melnyk, A. Wong, S. F. Bailey, 1155
1095 *et al.*, 2012 Evolutionary insight from whole-genome sequenc- 1156
1096 ing of experimentally evolved microbes. *Molecular ecology 1157*
1097 **21**: 2058–2077. 1158

1098 Fisher, R. A., 1918 The correlation between relatives on the sup- 1159
1099 position of mendelian inheritance. *Transactions of the Royal 1160*
1099 Society of Edinburgh

1100 **52**: 399–433. 1161

1101 Fisher, R. A., 1930 *The genetical theory of natural selection*. Claren- 1162
1102 don Press, London. 1163

1103 Gerstein, A. C., D. S. Lo, and S. P. Otto, 2012 Parallel genetic 1164
1104 changes and nonparallel gene–environment interactions char- 1165
1105 acterize the evolution of drug resistance in yeast. *Genetics 1166*
1106 **192**: 241–252. 1167

1107 Gerstein, A. C., J. Ono, D. S. Lo, M. L. Campbell, A. Kuzmin, 1168
1108 *et al.*, 2015 Too much of a good thing: the unique and repeated 1169
1109 paths toward copper adaptation. *Genetics* **199**: 555–571. 1170

1110 Gifford, D. R., E. Berriés-Caro, C. Joerres, T. Galla, and C. G. 1171
1111 Knight, 2019 Mutators drive evolution of multi-resistance to 1172
1112 antibiotics. *bioRxiv* p. 643585. 1173

1113 Gomulkiewicz, R. and R. D. Holt, 1995 When does evolution by 1174
1114 natural selection prevent extinction? *Evolution* **49**: 201–207. 1175

1115 Haldane, J. B. S., 1927 *A Mathematical Theory of Natural and 1176*
1116 Artificial Selection, Part V: Selection and Mutation. *Mathemat- 1177*
1117 ical Proceedings of the Cambridge Philosophical Society

1118 **23**: 838. 1178

1119 Harmand, N., R. Gallet, R. Jabbour-Zahab, G. Martin, and 1180
1120 T. Lenormand, 2017 Fisher’s geometrical model and the muta- 1181
1121 tional patterns of antibiotic resistance across dose gradients. 1182
1122 Evolution

1123 **71**: 23–37. 1183

1124 Iwasa, Y., F. Michor, and M. A. Nowak, 2004a Evolutionary dy- 1184
1125 namics of invasion and escape. *Journal of Theoretical Biology 1185*
1126 **226**: 205–214. 1186

1127 Iwasa, Y., F. Michor, and M. A. Nowak, 2004b Stochastic tunnels 1187
1128 in evolutionary dynamics. *Genetics* **166**: 1571–1579. 1188

1129 Jochumsen, N., R. L. Marvig, S. Damkær, R. L. Jensen, W. Paulan- 1189
1130 der, *et al.*, 2016 The evolution of antimicrobial peptide re- 1190
1131 sistance in *pseudomonas aeruginosa* is shaped by strong 1191
1132 epistatic interactions. *Nature communications* **7**: 13002. 1192

1133 Kassen, R. and T. Bataillon, 2006 Distribution of fitness effects 1193
1134 among beneficial mutations before selection in experimental 1194
1135 populations of bacteria. *Nature genetics* **38**: 484. 1195

1136 Kimura, M., 1965 A stochastic model concerning the mainte- 1196
1137 nance of genetic variability in quantitative characters. *Pro- 1197*
1138 ceedings of the National Academy of Sciences

1139 **54**: 731–736. 1198

1140 Kimura, M., 1983 *The neutral theory of molecular evolution*. Cam- 1199
1141 bridge University Press, Cambridge, UK. 1200

1142 Lande, R., 1980 The genetic covariance between characters main- 1201
1143 tained by pleiotropic mutations. *Genetics* **94**: 203–215. 1202

1144 Lindsey, H. A., J. Gallie, S. Taylor, and B. Kerr, 2013 Evolution- 1203
1145 ary rescue from extinction is contingent on a lower rate of 1204
1146 environmental change. *Nature* **494**: 463–467. 1205

1147 Luria, S. E. and M. Delbrück, 1943 Mutations of bacteria from 1148
1149 virus sensitivity to virus resistance. *Genetics* **28**: 491.

1150 MacLean, R. C. and A. Buckling, 2009 The distribution of fitness 1151
1152 effects of beneficial mutations in *Pseudomonas aeruginosa*. *PLoS 1153*
1154 Genetics

1155 **5**: e1000406.

1156 MacLean, R. C., A. R. Hall, G. G. Perron, and A. Buckling, 2010 1157
1157 The population genetics of antibiotic resistance: integrating 1158
1158 molecular mechanisms and treatment contexts. *Nature Re- 1159*
1159 views Genetics

1160 **11**: 405.

1161 Mao, E. F., L. Lane, J. Lee, and J. H. Miller, 1997 Proliferation 1162
1162 of mutators in a cell population. *Journal of Bacteriology* **179**: 1163
1163 417–422.

1164 Martin, G., 2014 Fisher’s geometrical model emerges as a prop- 1165
1165 erty of complex integrated phenotypic networks. *Genetics* **197**: 1166
1166 237–255.

1167 Martin, G., R. Aguilee, J. Ramsayer, O. Kaltz, and O. Ronce, 2013 1167
1168 The probability of evolutionary rescue: towards a quantitative 1169
1169 comparison between theory and evolution experiments. *Philosophical 1170*
1170 Transactions of the Royal Society of London B: Biological Sciences

1171 **368**: 20120088.

1172 Martin, G. and T. Lenormand, 2006 The fitness effect of muta- 1173
1173 tions across environments: a survey in light of fitness land- 1174
1174 scape models. *Evolution* **60**: 2413–2427.

1175 Martin, G. and T. Lenormand, 2015 The fitness effect of muta- 1176
1176 tions across environments: Fisher’s geometrical model with 1177
1177 multiple optima. *Evolution* **69**: 1433–1447.

1178 Martin, G. and L. Roques, 2016 The nonstationary dynamics of 1179
1179 fitness distributions: asexual model with epistasis and stand- 1180
1180 ing variation. *Genetics* **204**: 1541–1558.

1181 Maruyama, T. and M. Kimura, 1974 A note on the speed of gene 1182
1182 frequency changes in reverse directions in a finite population. 1183
1183 Evolution pp. 161–163.

1184 Ono, J., A. C. Gerstein, and S. P. Otto, 2017 Widespread genetic 1185
1185 incompatibilities between first-step mutations during parallel 1186
1186 adaptation of *saccharomyces cerevisiae* to a common environ- 1187
1187 ment. *PLoS biology* **15**: e1002591.

1188 Orr, H. A., 1998 The Population Genetics of Adaptation: The 1189
1189 Distribution of Factors Fixed during Adaptive Evolution. *Evolution* **52**: 935.

1190 Orr, H. A., 2005 The genetic theory of adaptation: a brief history. 1191
1191 *Nature Reviews Genetics* **6**: 119–27.

1192 Orr, H. A. and A. J. Betancourt, 2001 Haldane’s sieve and adap- 1193
1193 tation from the standing genetic variation. *Genetics* **157**: 875– 1194
1194 884.

1195 Orr, H. A. and R. L. Unckless, 2014 The population genetics of 1196
1196 evolutionary rescue. *PLoS Genetics* **10**: e1004551.

1197 Otto, S. P. and M. C. Whitlock, 1997 The probability of fixation 1198
1198 in populations of changing size. *Genetics* **146**: 723–733.

1199 Pennings, P. S., S. Kryazhimskiy, and J. Wakeley, 2014 Loss and 1200
1200 recovery of genetic diversity in adapting populations of hiv. *PLoS 1201*
1201 Genetics

1202 **10**: e1004000.

1203 Robbins, N., T. Caplan, and L. E. Cowen, 2017 Molecular evolu- 1204
1204 tion of antifungal drug resistance. *Annual Review of Microbiol- 1205*
1205 ogy

1206 **71**: 753–775.

1207 San Millan, A., J. A. Escudero, D. R. Gifford, D. Mazel, and R. C. 1208
1208 MacLean, 2017 Multicopy plasmids potentiate the evolution 1209
1209 of antibiotic resistance in bacteria. *Nature ecology & evolution* 1210
1210 **1**: 0010.

1211 Schlotterer, C., R. Kofler, E. Versace, R. Tobler, and S. Franssen, 1212
1212 2015 Combining experimental evolution with next-generation 1213
1213 sequencing: a powerful tool to study adaptation from stand- 1214
1214 ing genetic variation. *Heredity* **114**: 431–440.

1206 Stapley, J., J. Reger, P. G. Feulner, C. Smadja, J. Galindo, *et al.*, 1260
 1207 2010 Adaptation genomics: the next generation. *Trends in* 1261
 1208 *ecology & evolution* **25**: 705–712. 1262
 1209 Tenaillon, O., 2014 The utility of Fisher’s geometric model in 1263
 1210 evolutionary genetics. *Annual Review of Ecology, Evolution,* 1264
 1211 *and Systematics* **45**: 179–201. 1265
 1212 Tenaillon, O., F. Taddei, M. Radman, and I. Matic, 2001 Second- 1266
 1213 order selection in bacterial evolution: selection acting on mu- 1267
 1214 tation and recombination rates in the course of adaptation. 1268
 1215 *Research in microbiology* **152**: 11–16. 1269
 1216 Tenaillon, O., B. Toupance, H. Le Nagard, F. Taddei, and 1270
 1217 B. Godelle, 1999 Mutators, population size, adaptive land- 1271
 1218 scape and the adaptation of asexual populations of bacteria. 1272
 1219 *Genetics* **152**: 485–493. 1273
 1220 Turelli, M., 1984 Heritable genetic variation via mutation- 1274
 1221 selection balance: Lerch’s zeta meets the abdominal bristle. 1275
 1222 *Theoretical population biology* **25**: 138–193. 1276
 1223 Turelli, M., 1985 Effects of pleiotropy on predictions concerning 1277
 1224 mutation-selection balance for polygenic traits. *Genetics* **111**: 1278
 1225 165–195. 1279
 1226 Uecker, H. and J. Hermisson, 2016 The role of recombination in 1280
 1227 evolutionary rescue. *Genetics* **202**: 721–732. 1281
 1228 Uecker, H., S. P. Otto, and J. Hermisson, 2014 Evolutionary rescue 1282
 1229 in structured populations. *The American Naturalist* **183**: E17– 1283
 1230 E35. 1284
 1231 Weinreich, D. M., N. F. Delaney, M. A. DePristo, and D. L. Hartl, 1285
 1232 2006 Darwinian evolution can follow only very few mutational 1286
 1233 paths to fitter proteins. *science* **312**: 111–114. 1287
 1234 Weissman, D. B., M. M. Desai, D. S. Fisher, and M. Feldman, 2009 1288
 1235 The rate at which asexual populations cross fitness valleys. 1289
 1236 *Theoretical Population Biology* **75**: 286–300. 1290
 1237 Weissman, D. B., M. W. Feldman, and D. S. Fisher, 2010 The rate 1291
 1238 of fitness-valley crossing in sexual populations. *Genetics* **186**: 1292
 1239 1389–1410. 1293
 1240 Williams, K.-A. and P. S. Pennings, 2019 Drug resistance evolution 1294
 1241 in hiv in the late 1990s: hard sweeps, soft sweeps, clonal 1295
 1242 interference and the accumulation of drug resistance mutations. *BioRxiv* p. 548198. 1296
 1243 Wolfram Research Inc., 2012 *Mathematica*, Version 9.0. Champaign, IL. 1297
 1244 Yilmaz, N. K., R. Swanson, and C. A. Schiffer, 2016 Improving 1298
 1245 viral protease inhibitors to counter drug resistance. *Trends in* 1299
 1246 *Microbiology* **24**: 547–557. 1299
 1247

1249 Appendix

1250 Approximating the probability of 1-step rescue

1251 The probability of 1-step rescue in this model has been derived 1252
 1253 by [Anciaux *et al.* \(2018\)](#). As replicated in File S1 and given by
 1254 their equation 7, when $\rho_{max} = m_{max}/\lambda$ is large a simple, nearly
 1255 closed-form approximation is

$$\Lambda_1(m_0) \approx \tilde{\Lambda}_1(m_0) \equiv -m_0 U \frac{(1 - \psi_0/2)^{(1-n)/2}}{1 - \psi_0/4} g(\alpha), \quad (19)$$

1255 where $\psi_0 = 2(1 - \sqrt{1 - m_0/m_{max}})$, $g(\alpha) = \exp(-\alpha)/\sqrt{\pi\alpha} -$
 1256 $\text{erfc}(\sqrt{\alpha})$, and $\alpha = \rho_{max}\psi_0^2/4$, with $\text{erfc}(.)$ the complimentary
 1257 error function. When the wildtype declines slowly m_0 and thus
 1258 ψ_0 is small and $\Lambda_1(m_0) \approx U g(\alpha)$. In the limit $m_0 \rightarrow 0$, Equation
 1259 becomes

$$\tilde{\Lambda}_1(0) \equiv \lim_{m_0 \rightarrow 0} \tilde{\Lambda}_1(m_0) = 2U \sqrt{m_{max}\lambda/\pi}. \quad (20)$$

1260 *Mutant lineage dynamics*

1261 Here we follow the lead of [Weissman *et al.* \(2010\)](#) and [Uecker](#)
 1262 and [Hermisson \(2016\)](#) in approximating our discrete-time process
 1263 with a continuous-time branching process (see chapter 6 in
 1264 [Allen 2010](#)). Consider a birth-death process, where individuals
 1265 give birth at rate b and die at rate d . One can then obtain the
 1266 probability generating function for the number of individuals at
 1267 a given time, $n(t)$, given the initial number, $n(0)$. We are primarily
 1268 interested in new mutant lineages, $n(0) = 1$. The generating
 1269 function then allows us to calculate the probability that a lineage
 1270 persists at least until time t and the distribution of $n(t)$ given it
 1271 does so (see below).

1272 To convert between birth and death rates and our compound
 1273 Malthusian parameter we follow [Uecker and Hermisson \(2016\)](#)
 1274 in equally distributing the growth rate m between birth and
 1275 death, $b = (1 + m)/2$ and $d = (1 - m)/2$, such that $m = b - d$ and
 1276 the continuous-time process exhibits the same amount of drift
 1277 as the discrete time process (and matches discrete-time
 1278 simulations well; [Uecker *et al.* 2014](#)). We can now report the
 1279 necessary results in terms of m (assuming $|m| < 1$).

1280 Denoting the extinction time as T , the probability a mutant with
 1281 growth rate m persists until time t is approximately (see File S1 for derivation)

$$P(T > t) \approx \begin{cases} 2/t & t \ll |1/m| \\ -2m \exp(mt) & t \gg -1/m > 0 \end{cases} \quad (21)$$

1282 As pointed out in [Weissman *et al.* \(2010\)](#) (whose equation A2
 1283 differs from Equation 21 by a factor of 2 because they have
 1284 $b + d = 2$), the distribution of persistence times has a long
 1285 tail (like $1/t$) until being cut off (declining exponentially) at
 1286 $t = -1/m$.

1287 Given a lineage persists until t , the distribution of $n(t)$ is
 1288 roughly (see File S1 for derivation)

$$P(n(t) = n | n(t) > 0) \approx \begin{cases} 2(1/t)(1 + 2/t)^{-n} & t \ll |1/m| \\ -2m(1 + m)^{n-1} & t \gg -1/m > 0 \end{cases} \quad (22)$$

1289 As pointed out in [Weissman *et al.* \(2010\)](#) (whose equation A3
 1290 only differs from Equation 22 by constants), the distribution of
 1291 $n(t)$ is approximately geometric for small or large t , implying
 1292 $n(t)$ is very unlikely to be greater than the minimum of t and
 1293 $-1/m$.

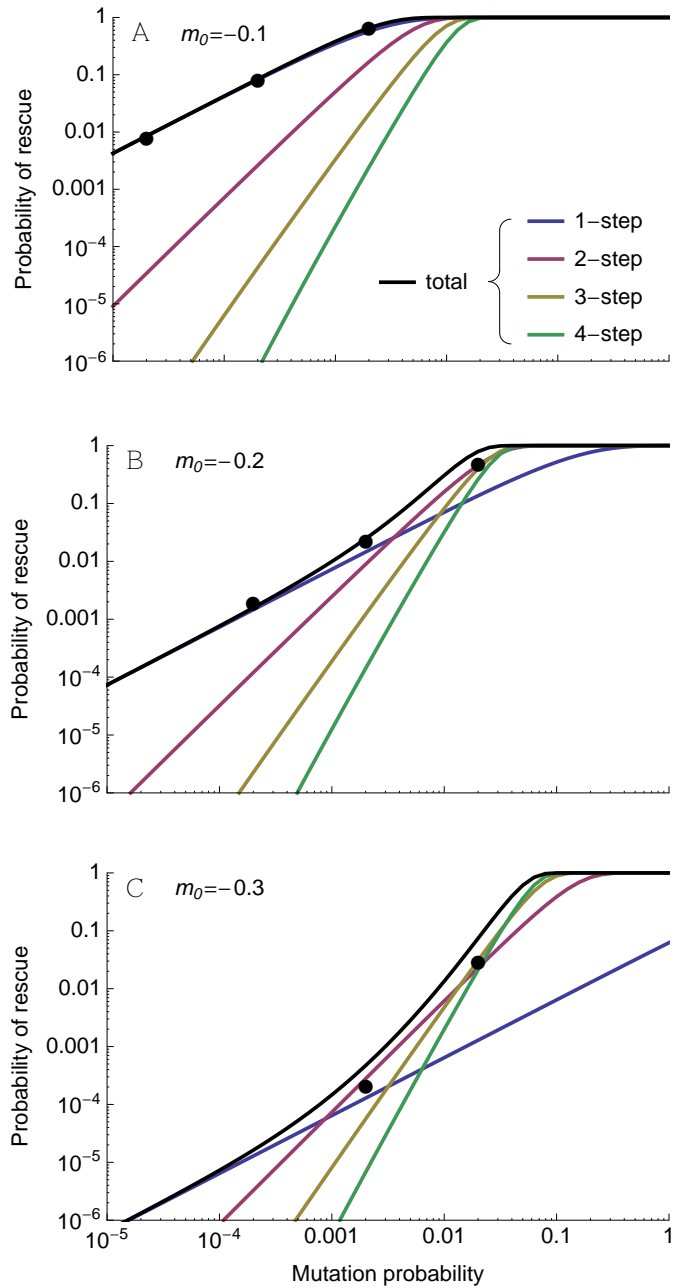


Figure S1 The probability of rescue as a function of mutation rate for three different levels of initial maladaptation. See Figure 3 for details. Other parameters: $n = 4$, $\lambda = 0.005$, $m_{max} = 0.5$, $N_0 = 10^4$.

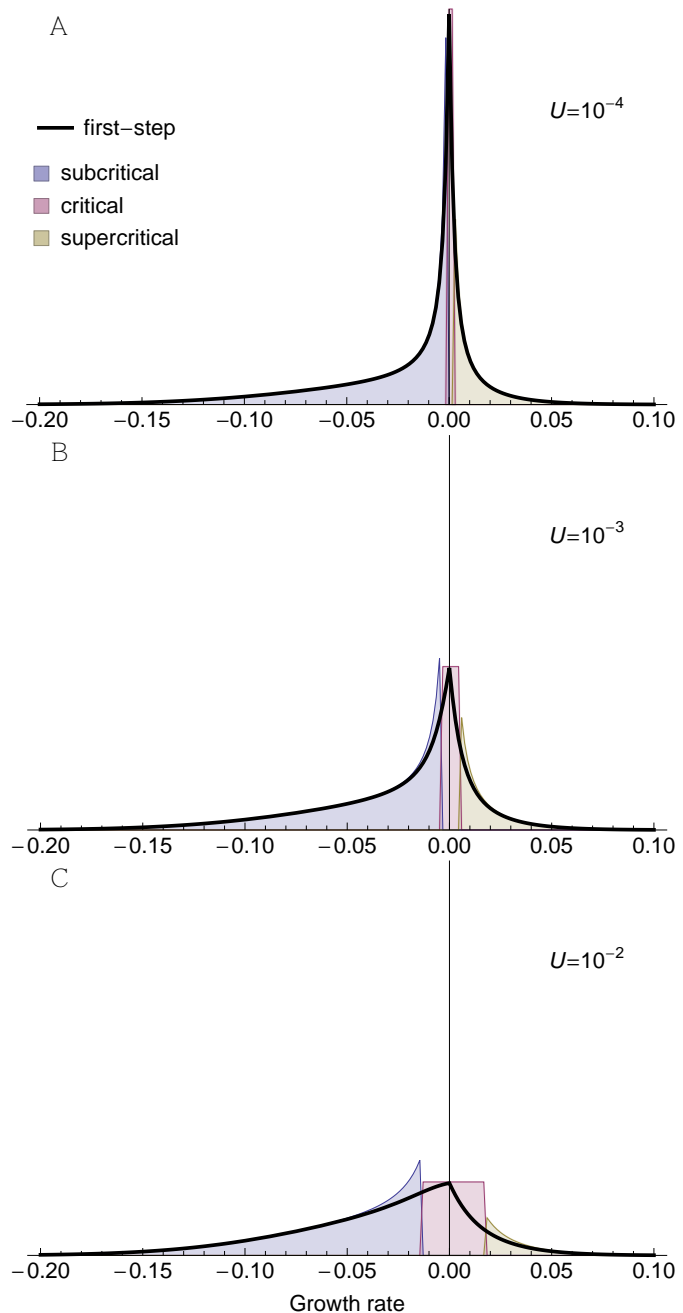


Figure S2 The distribution of first-step mutant growth rates given 2-step rescue under three mutation rates. See Figure 7 for details. Parameters: $n = 4$, $\lambda = 0.005$, $m_{max} = 0.5$, $m_0 = -0.2$.

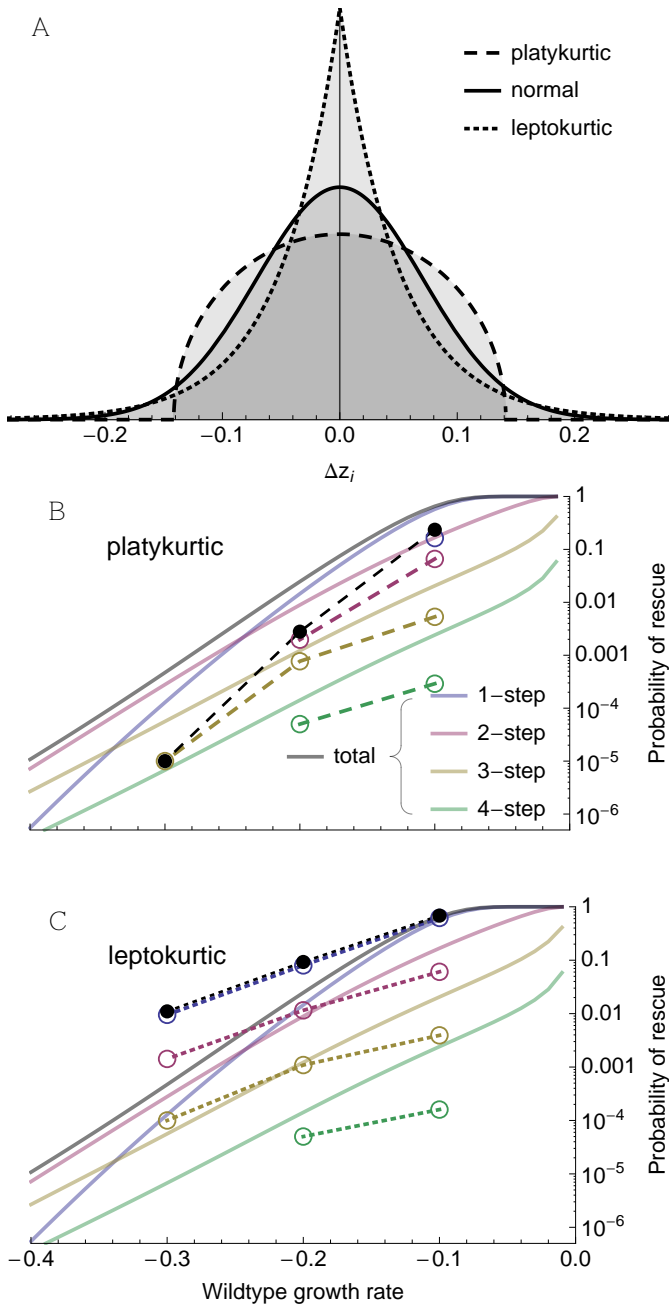


Figure S3 (A) One-dimensional slices of multidimensional platykurtic (dashed; semicircle), normal (solid; as used in main text), and leptokurtic (dotted; Laplace) mutational distributions with the same (co)variance but varying kurtosis. (B,C) The probability of 1-, 2-, 3-, or 4-step rescue with platykurtic and leptokurtic mutational distributions, respectively. The dots and broken lines represent simulation results (10^5 replicates for each wildtype growth rate). The solid lines are the numerical results for the normal mutational distribution (as in Figure 3). Parameters: $N_0 = 10^4$, $U = 2 \times 10^{-3}$, $n = 4$, $\lambda = 0.005$, $m_{max} = 0.5$.

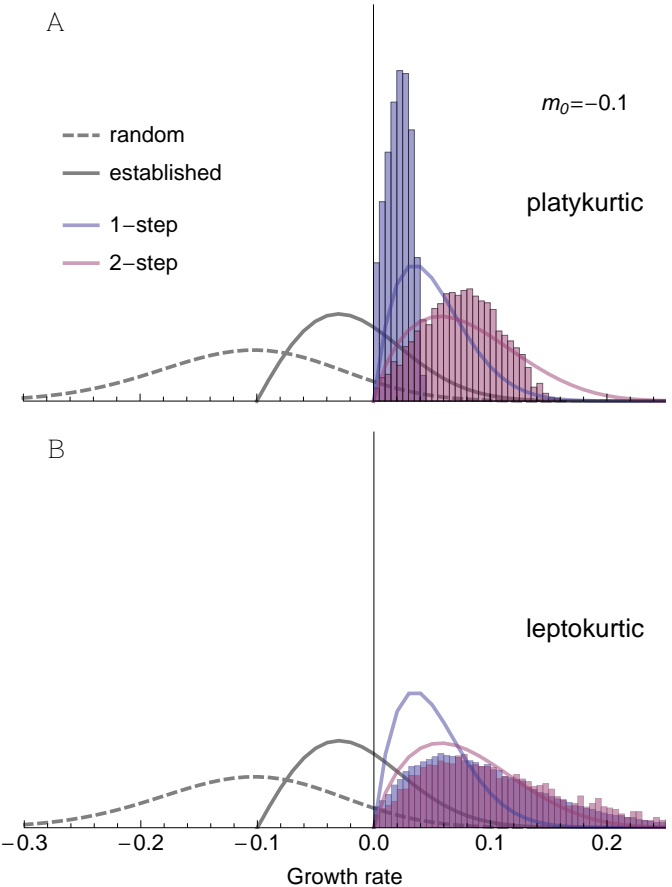


Figure S4 The distribution of growth rates among rescue genotypes under 1-step (blue) and 2-step (red) rescue with (A) platykurtic and (B) leptokurtic mutational distributions (see Figure S3A). The solid lines are predictions for a normal mutational distribution (as in Figure 6). The histograms show the distribution of growth rates among rescue genotypes observed across 10^5 replicate simulations. Parameters: $N_0 = 10^4$, $U = 2 \times 10^{-3}$, $n = 4$, $\lambda = 0.005$, $m_{max} = 0.5$, $m_0 = -0.1$.

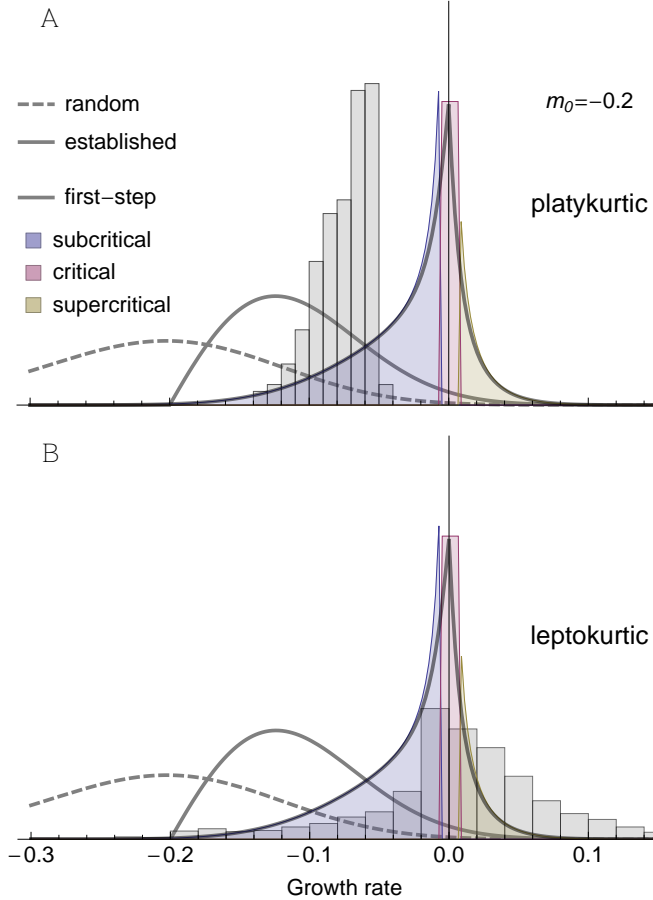


Figure S5 The distribution of growth rates among first-step mutations that lead to 2-step rescue with (A) platykurtic and (B) leptokurtic mutational distributions (see Figure S3A). The curves and shadings are predictions for a normal mutational distribution (as in Figure 7). The histograms show the distribution of growth rates observed across 10^5 replicate simulations. Parameters: $N_0 = 10^4$, $U = 2 \times 10^{-3}$, $n = 4$, $\lambda = 0.005$, $m_{max} = 0.5$, $m_0 = -0.2$.

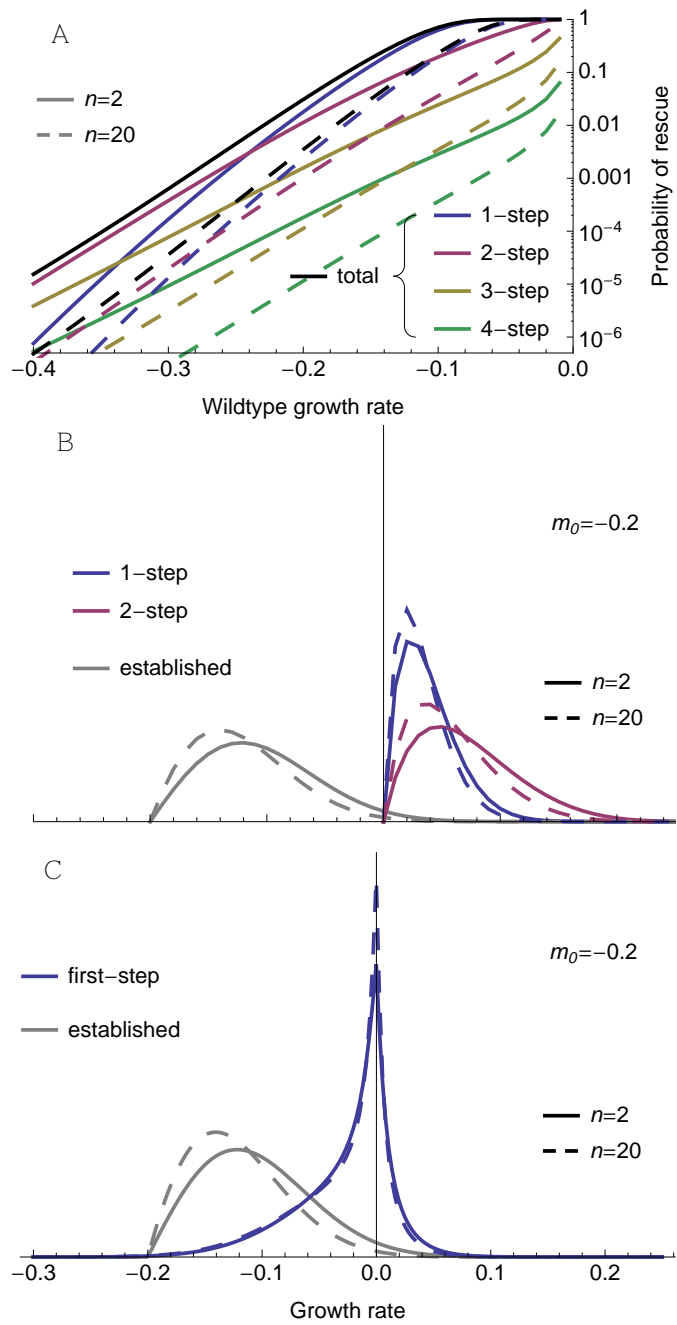


Figure S6 The effect of the number of phenotypic dimensions, n , on (A) the probability of k -step rescue, (B) the distribution of growth rates among rescue genotypes, and (C) the distribution of growth rates among first-step mutants that lead to 2-step rescue. Curves are numerical results, as in Figures 3, 6, and 7. Parameters: $N_0 = 10^4$, $U = 2 \times 10^{-3}$, $\lambda = 0.005$, $m_{max} = 0.5$.